Renewable Energy 114 (2017) 1160–1179

Contents lists available at ScienceDirect

Renewable Energy

journal homepage: www.elsevier.com/locate/renene

Multi-scale ocean response to a large tidal stream turbine array

Michela De Dominicis [a, *], Rory O'Hara Murray [b], Judith Wolf [a]

[a] National Oceanography Centre, 6 Brownlow Street, Liverpool L3 5DA, United Kingdom
[b] Marine Scotland Science, Scottish Government, 375 Victoria Road, Aberdeen AB11 9DB, United Kingdom

ARTICLE INFO

Article history:
Received 13 January 2017
Received in revised form
10 July 2017
Accepted 12 July 2017
Available online 14 July 2017

Keywords:
Tidal stream energy
Marine renewable energy
Tidal stream turbine array
Pentland Firth
NW European Shelf
FVCOM

ABSTRACT

The tidal stream energy sector is now at the stage of deploying the world's first pre-commercial arrays of multiple turbines. It is time to study the environmental effects of much larger full-size arrays, to scale and site them appropriately. A theoretical array of tidal stream turbines was designed for the Pentland Firth (UK), a strait between Scotland and the Orkney Islands, which has very fast tidal currents. The practical power resource of a large array spanning the Pentland Firth was estimated to be 1.64 GW on average. The ocean response to this amount of energy extraction was simulated by an unstructured grid three-dimensional FVCOM (Finite Volume Community Ocean Model) and analysed on both short-term and seasonal timescales. Tidal elevation mainly increases upstream of the tidal array, while a decrease is observed downstream, along the UK east coast. Tidal and residual flows are also affected: they can slow down due to the turbines action or speed up due to flow diversion and blockage processes, on both a local and regional scale. The strongest signal in tidal velocities is an overall reduction, which can in turn decrease the energy of tidal mixing and perturb the seasonal stratification on the NW European Shelf.

1. Introduction

The ocean can be a source of energy: from waves, tides, ocean currents, salinity and thermal gradients [1,2]. Presently, marine renewable energy mainly considers tidal and wave energy devices [3], which have the benefit of being scalable. Tidal energy, driven by gravitational forces of the moon and the sun, has the distinct advantage over wave energy of being highly predictable [4]. Tidal energy has two components, the potential energy due to the sea level variations (tidal range), and the kinetic energy of the tidal currents. Potential energy can be exploited using tidal barrages or tidal lagoons to create sea water level differences, while kinetic energy of the fluid movement generated by tidal currents can be extracted using a suitable underwater type of turbine rotor. Although being called "tidal stream turbines", it has to be noted that a turbine placed in the ocean extracts energy from the total incoming ocean current, which is composed of wind driven and density driven currents, as well as tidal currents.

The world's first marine energy test facility was established in 2003 to kick-start the development of the wave and tidal energy industry in Europe. Based in Orkney, Scotland, the European Marine Energy Centre (EMEC) has provided a variety of test sites in real sea conditions. In recent years, several prototypes of tidal stream turbines have successfully generated electricity and delivered it into the grid at the EMEC site and other locations, thus proving the concept: e.g. Open-Centre Turbine (OpenHydro) in 2006, SeaGen (Marine Current Turbines) in 2008, HS1000 (Andritz Hydro Hammerfest) in 2012, Nova M100 (Nova Innovation) in 2016 and AR1500 (Atlantis Resources Corp) in 2017. Next, the tidal stream energy sector will deploy front-runner technologies in arrays of multiple devices to generate more significant amounts of electricity, and prove that it can work on a commercial scale. MeyGen tidal energy project and Nova Innovation are now installing some of the world's first pre-commercial arrays off Caithness and Shetland (Scotland, UK). MeyGen uses turbines from Atlantis and Andritz Hydro Hammerfest, while Nova Innovation uses their own devices.

It is important that marine renewable energy is developed in a sustainable and socially responsible manner that will not harm the marine environment either directly or in combination with other marine activities. The effects that tidal turbines may have on the marine environment can depend on the device design, location, animals and habitat present and scale of development. While potential environmental impacts of tidal barrages has been more extensively studied in the past [5], showing locally a general loss of intertidal habitat within the impounded basins, present knowledge of how tidal current turbines interact with the marine environment is limited. The concern about localised effects, such as habitat loss

* Corresponding author.
E-mail address: micdom@noc.ac.uk (M. De Dominicis).

http://dx.doi.org/10.1016/j.renene.2017.07.058

or degradation, acoustic effects and collision risk of marine mammals, fish, and seabirds, was the primary one, with pioneering studies of Refs. [6,7] and [8]. However, no collisions have been observed around single turbines or small arrays as reported in more recent studies [9]. The effects of increasing noise levels from tidal turbines are less understood, partly because the undisturbed behavioural ecology of many marine animals is poorly understood. However, to date, there have been no observations of operational noise from tidal devices affecting marine animals [9]. Effects on the local flow, at the scale of the single device and near-field < 1 km, are often investigated as part of the design procedure, by means of laboratory or modelling studies [10–13]. Those effects include flow deceleration/acceleration and modification of intensity and spatial variability of turbulence around the devices, which in turn affect scouring and resuspension/accumulation of sediments [14].

On the other hand, very little is known about region-wide impacts of energy extraction by large arrays of tidal stream turbines. Extracting any form of ocean energy leaves less energy in the ocean system, and the environmental impact of energy extraction is not necessarily restricted to the vicinity of the turbine site. Effects on the physical marine environment, that are going to be examined in this work, include changes in sea surface elevation, water temperature, salinity, stratification, marine currents, which can then affect the associated transport of sediments, nutrients and microorganisms. Understanding those possible impacts and the mechanisms behind them might help in the exploitation of tidal energy without harming the marine environment, e.g. if tidal turbine farms are scaled and sited appropriately.

Field studies focusing on energy removal effects and changes in flow caused by tidal stream turbines are not possible until commercial sized arrays are deployed and operated for a period of years. Thus, hydrodynamic models can help in understanding how tidal stream turbines and energy removal will influence flow conditions. Studies are starting to emerge modelling the energy removal by tidal stream turbines and focusing on far-field environmental effects in different world locations (see Table 1). State-of-the-art studies are mainly focused on the effects of energy removal on hydrodynamics and associated sediment transport, looking at spatial scales between 1 and 100 km from the tidal arrays. To date, only a few studies [17,28,30] have focused on very far-field effects (> 100 km). When examining the changes in hydrodynamics, previous work has mainly focused on tidal circulation and water level, usually covering the temporal scale of a spring-neap cycle. Two studies have however included wind-driven and density driven ocean currents in the model setup in order to study changes in residual currents on a temporal scale of 2 months [29] and effects on circulation and associated effects on biogeochemistry on a scale of 6 months [17].

Structured grid three-dimensional (3D) models have been widely used [17,26–29] to study far-field environmental impacts. However, the disparity of scales between the turbine and the size of the coastal model domain may benefit from the use of unstructured model grids, in order to have high resolution close to the array location and low resolution in the broader model domain. The computational effort for unstructured grid models can be challenging and can be significantly reduced by using a depth-averaged or two-dimensional (2D) numerical model [19,20,22,24,30]. Depth-averaged models, by their definition, will impose changes due to tidal turbines through the entire water column with possible overestimation of extracted energy and misrepresentation of effects [15], whose estimates are dependent on the vertical cross sectional area that is considered to be occupied by tidal turbines and on the modification of the surface and bottom flow fields. Some 3D unstructured grid models have already been used [16,18,21],

Table 1
State-of-the-art modelling studies of far-field environmental effects of tidal stream energy removal (all studies listed include a parameterisation of tidal energy extraction).

Reference	Tidal array location	Effects on	Spatial and temporal scale	Hydro Model Setup
this study	Pentland Firth (UK)	Hydrodynamics	> 100 km - 1 year	3D FVCOM - Unstructured grid (750 m - 20 km)
[15]	Pentland Firth (UK)	Hydrodynamics (tides only)	[1 km - 100 km] - spring-neap cycle	3D ROMS - Structured grid (500 m)
[16]	Pentland Firth (UK)	Hydrodynamics (tides only)	[1 km - 100 km] - 12.42 h	3D FVCOM - Unstructured grid (150 m - 3 km)
[17]	Pentland Firth (UK)	Hydrodynamics; Biogeochemistry	> 100 km - 6 months	3D GETM-ERSEM - Structured grid (5 km)
[18]	Pentland Firth (UK)	Hydrodynamics (tides only); Sediments	[1 km - 100 km] - 2 spring-neap cycles	3D MIKE - Unstructured grid
[19]	Pentland Firth (UK)	Sediments	[1 km - 100 km] - 2 spring-neap cycles	2D Fluidity - Unstructured grid (18 m - 20 km)
[20]	Alderney Race (France)	Hydrodynamics (tides only); Sediments	[1 km - 100 km] - 2 spring-neap cycles	2D Telemac - Unstructured grid (150 m - 10 km)
[21]	Tacoma Narrows, Washington (USA)	Hydrodynamics (tides only)	[1 km - 100 km] - 2 spring-neap cycles	3D FVCOM - Unstructured grid (30 m - 200 m)
[22]	Anglesey - Irish Sea (UK)	Sediments	[1 km - 100 km] - 2 spring-neap cycles	2D Telemac - Unstructured grid (15 m - 2 km)
[23]	Ria de Ribadeo - Galicia (Spain)	Hydrodynamics	[1 km - 100 km] - spring-neap cycle	3D Delft (depth-averaged) - Structured grid (5 m - 150 m)
[24]	Tory Channel (New Zealand)	Hydrodynamics (tides only)	[1 km - 100 km] - 12.42 h	2D RICOM - Unstructured grid (25 m - 4 km)
[25]	Bristol Channel (UK)	Hydrodynamics (tides only); Sediments; Water Quality	[1 km - 100 km] - spring-neap cycle	2D DIVAST - Structured grid (200 m/ 600 m)
[26]	Alderney Race (France)	Hydrodynamics (tides only); Sediments	[1 km - 100 km] - spring-neap cycle	3D POLCOMS (depth-averaged) - Structured grid (150 m)
[27]	Georgia coast (USA)	Hydrodynamics (tides only)	[1 km - 100 km] - spring-neap cycle	3D ROMS (Regional Ocean Modeling System)- Structured grid (180 m - 330 m)
[28]	Minas Passage (Canada)	Hydrodynamics (tides only)	> 100 km - 2 spring-neap cycles	3D POM - Structured grid (1.5 km/ 4.5 km)
[29]	Eastern Celtic Sea (UK)	Hydrodynamics	[1 km - 100 km] - 2 months	3D POLCOMS - Structured grid (2 km)
[30]	Minas Passage (Canada)	Hydrodynamics (tides only)	> 100 km	2D FVCOM - Unstructured grid

however, in their implementation they neglected wind- and density- driven currents.

This paper focuses on the potential effects on hydrodynamics caused by realistic large arrays of tidal stream turbines, which should be first examined to scale and site them appropriately. A pioneering area of research in the context of marine renewable energies is in the Pentland Firth (UK), a channel between the Scottish mainland and the Orkney Islands (see Fig. 1-A) with very high tidal velocities and in which tidal stream turbines have already been placed for testing in real sea conditions. It has been suggested that the UK has 32 GW of tidal stream power, with 11 GW in Scottish Waters, and the most significant contribution of 6 GW from Pentland Firth and Orkney Waters (PFOW) [31]. Initial estimates of the tidal stream power in the Pentland Firth vary considerably from approximately 1 GW averaged over a tidal cycle [32] to approximately 18 GW at peak flow [33]. These estimates are dependent on the vertical cross sectional area that is considered to be occupied by tidal turbines and most of them do not include the feedbacks of tidal energy extraction on the flow. Recently, Ref. [16] showed that the available power for electricity generation from the Pentland Firth through an M_2 tidal cycle peaks at 10.8 GW and has a mean value of 4.9 GW, including the feedbacks due to tidal stream energy extraction, but with the full vertical cross section of the Pentland Firth utilised. Since the latter is very unlikely, given the potential impact that such a scenario could have on the marine environment and other users (e.g. navigation), [16] further concluded that with turbines occupying only the bottom part of the water column, the mean power resource of an M_2 tidal cycle reaches a plateau around 1.53 GW.

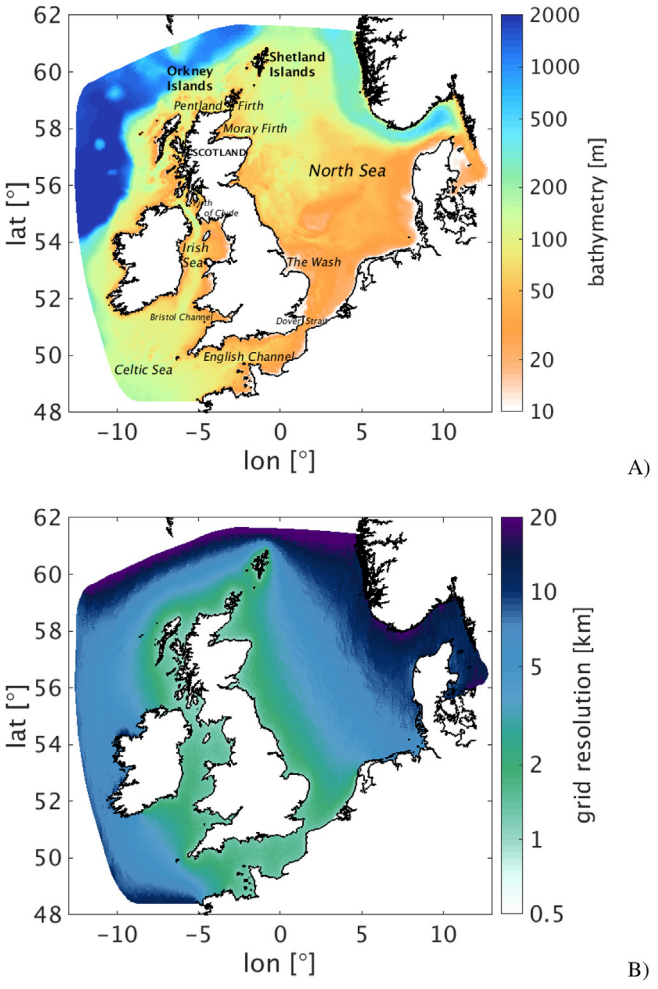

Fig. 1. Scottish Shelf Model (SSM) bathymetry and main shelf sea locations (A) and grid resolution (average horizontal node to node spacing) of the triangular model elements (B).

A comprehensive assessment of the tidal energy resource available for electricity generation and the study of the potential environmental impacts associated with its extraction in the Pentland Firth (UK) has been performed in this work and it can then lead the way to further development in other UK regions and different countries. In order to examine both local ($<$ 100 km) and region-wide ($>$ 100 km) spatial scales, the Scottish Shelf Model (SSM), an unstructured grid three-dimensional FVCOM (Finite Volume Community Ocean Model, [34] model implementation [35], is a useful tool, since it covers the entire NW European Shelf (see Fig. 1), but with a high resolution where the tidal stream energy is extracted. A large theoretical array of tidal stream turbines has been designed following a novel method, applicable to any other area, and has been implemented in the SSM using the momentum sink approach to represent the loss of momentum due to tidal energy extraction. An estimate of the available power for electricity generation from the Pentland Firth has been obtained including tidal stream energy extraction feedbacks on the flow and considering the realistic operation of a generic tidal stream turbine.

Near and far-field effects generated by tidal stream energy extraction in the Pentland Firth have been evaluated by comparing a set of ocean physical parameters describing the present ocean climate and the ocean state modified by tidal energy extraction. To extend the knowledge acquired in previous studies, the SSM model setup included atmospheric and freshwater forcings, enabling it to reproduce baroclinic (density-driven) and barotropic (mainly tidal and wind driven) circulation for a climatological year. Thus, we were able to look for changes in tidal circulation as well as possible changes in residual currents and ocean stratification: the latter has never been addressed in previous studies. Furthermore, the temporal scale covered by the model run is one year, allowing us for the first time to examine how tidal energy extraction can potentially interact with different seasonal hydrodynamic conditions.

The paper is organised as follows: Section 2 presents the methodology, which includes a description of the FVCOM Scottish Shelf Model, the parameterisation used to reproduce the energy extraction due to the operation of tidal stream turbines and a description of the scenario analysed; Section 3 presents the results; Section 4 discusses the major findings, study's limitations and future research and Section 5 briefly summarises our conclusions.

2. Methodology

2.1. Scottish Shelf Model

The Scottish Shelf Model (SSM) is an implementation of the unstructured grid, finite-volume, three-dimensional (3D) hydrodynamic model FVCOM (Finite Volume Community Ocean Model, [34]). The overall study area includes the NW European Shelf from 48°N to 62°N and 13°W to 13°E. The domain extends beyond the shelf to include some of the adjacent North-East Atlantic deep waters (see Fig. 1-A), but the focus of this model is on the Scottish shelf itself and deep waters are primarily included to ensure the model boundaries are far enough away so they do not interfere with the area of interest.

The FVCOM horizontal grid comprises unstructured triangular cells: the SSM model horizontal resolution is variable, with horizontal node to node spacing ranging from 10 to 20 km offshore down to 500 m - 1 km near the coast, the spatial resolution minimum allows to resolve tidal-stream energy sites [4]. The horizontal grid is

mainly refined in the Scottish shelf waters less than 200 m deep where the model is primarily focused (see Fig. 1-B). The model grid has been built starting from the Global Self-consistent, Hierarchical, High-resolution Shoreline (GSHHS) data for coastline. For the vertical discretisation FVCOM uses a σ coordinate system (terrain following coordinates), and the SSM implementation has 20 uniform σ layers. The SSM model bathymetry (see Fig. 1-A) was supplied by EMODnet and by the North-West Shelf Operational Oceanographic System (NOOS), the latter for the North Sea east of 0°E.

The vertical turbulent mixing scheme is the $k-\varepsilon$ turbulent closure model of General Ocean Turbulent Model (GOTM) [36], which can be coupled with FVCOM. For the horizontal mixing the Smagorinsky [37] parameterisation is used with a constant horizontal diffusivity value of 0.2 m^2/s. Bottom friction is calculated by means of a uniform roughness length applied to the whole domain, equal to 0.01 m (value tuned on the basis of validation against tide gauges and current meters data in Scottish Waters, see Ref. [35]. The drag coefficient in the quadratic drag law is fitted to a logarithmic boundary layer applied in the near-bed model level.

For this specific study we decided to perform a one year climatological mode run in order to represent a typical annual cycle. The model was forced with climatologically averaged conditions, including atmospheric forcing, and temperature and salinity at the open boundary and fresh water input from rivers along the coastline.

The climatological atmospheric forcing has been built from the monthly 1990-2014 ERA-Interim [38] data of mean sea level pressure, precipitation, evaporation, temperature, thermal/solar radiations and wind (for wind, daily data have been used). Sensible and latent heat fluxes are calculated by FVCOM using the COARE2.6 air-sea flux algorithm [39], which includes the cool-skin effect [40].

Ocean boundaries have been constructed using the monthly 1990-2014 data of temperature, salinity, currents and sea elevation provided by the Atlantic Margin Model 7 km (AMM7, [41,42]) simulation. AMM7 is a NEMO model [43] implementation for the NW European Shelf. Hourly water elevation and tidal currents are added on top of climatological currents and water elevation (a representative average tidal year has been selected, a climatological average has not been performed for tides). Tidal currents and water elevations along the open boundary were obtained for 8 tidal constituents (M_2, S_2, N_2, K_2, K_1, O_1, P_1, Q_1) from TPXO7.2, a global model of ocean tides based on the Oregon State University tidal inversion of TOPEX/POSEIDON and Jason altimeter data [44]. Current velocities (residual and tidal), temperature, salinity and water elevation, after being interpolated, are prescribed at all the nodes and elements of the FVCOM model boundary with a temporal resolution of 1 h.

Water elevation and currents are perturbed by tidal energy extraction, while the open boundary is forced by the undisturbed state. An impractical solution is to model the entire globe, but a reasonable compromise is to increase the domain of the model and to place the boundary beyond the edge of the continental shelf, so that the power extraction from the proposed site has a negligible effect at the edge of the domain [45,46].

The river runoff volume flux climatology were obtained from the Centre for Ecology and Hydrology (CEH) Grid-to-Grid (G2G) model [47–49], covering the period from 1962 to 2011 and including 577 rivers in Scottish Waters. Initial conditions are monthly climatological temperature and salinity from the AMM7 model; the model is started from rest using a spin-up time of 3 months (a longer spin-up time of 1 year has been tested, showing no significant changes in the results).

The results from the climatology run have been compared with climatological atlas information for temperature, salinity and currents. Although in this work we use climatological forcing, the model has been run for a specific period of time and water levels, currents and temperature and salinity have been validated against observed data. The model validation is presented in Ref. [35].

The SSM model has been run first for a climatological year, to have a baseline of the climatological seasonal conditions. Next, a tidal stream array located in the Pentland Firth has been introduced into the model using the approach described in Section 2.2 and the perturbed hydrodynamic conditions have been compared with the baseline.

2.2. Tidal stream turbines parameterisation

To be computationally viable, models of large arrays of turbines usually use a simplified representation of the turbines. Simplified parameterisations aim to reproduce the effects of the flow and turbulence around an idealised turbine to give a coarse representation of the hydrodynamic force on a turbine or a group of turbines. The most basic approximation for modelling power extraction is to enhance the natural bottom drag coefficient over the area spanned by the array, which is the approach widely used in the past to parameterise tidal energy extraction in 2D momentum equations [19,20,22,24,26,30]. In this work we use a momentum sink approach, in which a retarding force representing the loss of momentum due to tidal energy extraction is added to the 3D momentum equations [15–18,23,27–29].

The horizontal force applied by the fluid on a turbine is called the thrust force F_T and it is typically expressed as a quadratic drag law in the form:

$$\mathbf{F_T} = \frac{1}{2}\rho C_T A|\mathbf{u}|\mathbf{u} \tag{1}$$

where ρ is the water density, C_T is the thrust coefficient, $\mathbf{u}$ is the fluid velocity and A is the area swept by the turbine blades, assuming that the turbine is always oriented to face into the current, which is realistic as horizontal axis turbines can be designed with a yaw mechanism allowing the turbine to always face into the flow. The effect of energy extraction on the fluid is then simulated by implementing an additional retarding force equal and opposite to the thrust in the momentum equations.

FVCOM uses a mode-splitting approach in the numerical scheme to solve the depth-averaged 2D barotropic external model and 3D baroclinic internal mode equations; the momentum governing full equations with momentum sink terms due to energy extraction can be found in Refs. [50] and [16]. If we consider that (i) a tidal turbine occupies a single grid cell, (ii) a turbine can span multiple σ-layers and (iii) multiple turbines can be in one control element, the momentum sink terms at each level (3D internal mode, eq. (2)) and depth-integrated (2D external mode, eq. (3)) are:

$$\mathbf{F}(i,k) = -\frac{1}{2}\rho N(i) C_T(i) A K_\sigma(i,k)|\mathbf{u}(i,k)|\mathbf{u}(i,k) \tag{2}$$

$$\mathbf{F}(i) = -\frac{1}{2}\rho N(i) C_T(i) A \sum_{k=1}^{k=n} K_\sigma(i,k)|\mathbf{u}(i,k)|\mathbf{u}(i,k) \tag{3}$$

where $\mathbf{F}$ represents the force exerted on the fluid by the turbine, which is then expressed per unit of mass when added in the FVCOM momentum equations, i stands for the model element and k for the model σ-layer, $N(i)$ is the number of turbines in a model element, $K_\sigma(i,k)$ the fraction of the flow facing area occupied by the turbine in the k-th σ layer and n is the total number of σ layers. A simplified approach could be used considering the turbine as spanning the

entire water column and/or using the depth-averaged velocity, instead of the velocities in each layer occupied by a tidal turbine. However, this can lead to an overestimation of the extracted energy and of the impacts [16]. An additional momentum sink term due to the drag of the physical structures of turbine blades, supporting poles and foundations can also be potentially included [50], but has not been considered in this study.

The turbine thrust coefficient, C_T, can either be considered constant or more realistically varied as a function of the flow speed in order to reproduce the turbine operation, which is characterised by cut-in, cut-out and rated speed. Below the cut-in speed, the flow speed is insufficient to rotate the blades and the turbine generates no power. Between cut-in and rated speed, the turbine extracts power in proportion to the kinetic energy incident over its swept area. When the flow exceeds the rated speed, the power output reaches the limit that the electrical generator is capable of. The turbine will then be regulated with a way of limiting the power output and shedding mechanical load at high flow speeds, this reduces the thrust and hence the forces on the rotor and the structure. Above cut-out speed, the turbine is shut down to avoid damaging it. In this work, the generic (i.e. not for a specific turbine design) thrust coefficient curve constructed by Ref. [51] has been used, with a rated power of ≈ 2 MW, a cut-in speed of 1 m/s, a maximum rated speed of 2.5 m/s and a cut-out speed of 4 m/s. A sensitivity analysis to use of a constant or variable thrust coefficient is also shown in Section 3.1.

2.3. Tidal array design

The average power density (APD) for each element in the Pentland Firth was estimated from a 30-day SSM model run forced only by tides and without including any feedbacks of tidal arrays on the flow, using

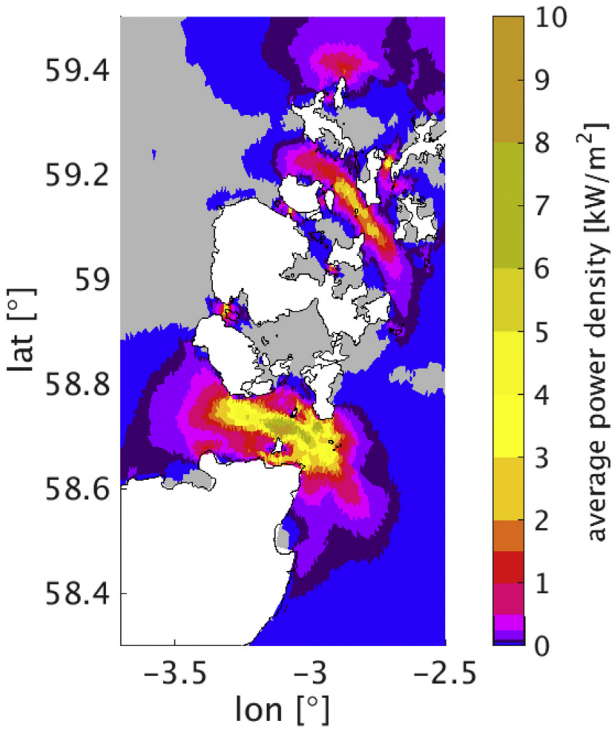

Fig. 2. Average power density [kW/m^2] in the Pentland Firth estimated from a 30 days SSM model run forced by 8 tidal constituents (M_2, S_2, N_2, K_2, K_1, O_1, P_1, Q_1), without including any feedbacks of tidal arrays on the flow.

$$APD(i) = \left\langle \frac{1}{2}\rho\overline{|\mathbf{u}(i,t)|}^3 \right\rangle_t \tag{4}$$

where $\overline{|\mathbf{u}(i,t)|}$ is the depth-averaged tidal current speed, $\langle\,\rangle_t$ represent a time mean average over 30 days. APD is expressed as [kW/m^2] and it is the power density in a vertical plane perpendicular to the tidal current direction. Fig. 2 shows the APD in the Pentland Firth. The power [GW] that can be potentially generated is then the power density times the vertical cross-sectional area occupied by tidal stream turbines.

Whilst it is important to understand the total exploitable resource it is also important to understand and quantify more practical realistic and sustainable scenarios. In this work we consider three main limitations: (1) water depth; (2) capacity factor; (3) turbine spacing. First, the tidal turbine array designed in this work takes into account that it is unlikely that turbines would span the full water depth and horizontal axis turbines would not be placed in water depths less than the diameter of the turbine blades. This study uses a generic horizontal axis tidal turbine design developed in Ref. [51]; with 20 m diameter blades, which "weathervanes" into the tidal flow, and has a rated power of ≈ 2 MW. The hub height has been set to be 15 m above the bed. Thus, in this study turbines were placed in locations with water depths > 27.5 m, allowing them to remain submerged at all tidal states. Second, the array design is based on device utilisation, which can be quantified by the capacity factor, defined as the ratio of the APD (from the undisturbed resource) to the power density at the turbine rated speed [52]:

$$CF(i) = \frac{\left\langle \frac{1}{2}\rho\overline{|\mathbf{u}(i,t)|}^3 \right\rangle_t}{\frac{1}{2}\rho|\mathbf{u}_R(i)|^3}\,100 \tag{5}$$

where $|\mathbf{u}_R(i)|$ is the turbine rated speed (2.5 m/s, see Section 2.2). Feasibility studies indicate that the lowest cost of energy for tidal stream turbines would be achieved with capacity factors between 30% and 40% [53]. Third, a minimum lateral turbine spacing of 3 device widths and a minimum downstream spacing of 15 device widths, to eliminate wake effects [12], have been used.

Fig. 3-A shows the area (green line) identified in the Scottish Governments National Marine Plan as an area of search for future tidal stream energy development [54]. This initial area of search has been further reduced to three strips of tidal turbines across the central part of Pentland Firth, linking the Scottish mainland to the island of Stroma, Swona and South Ronaldsay (white enclosed areas in Fig. 3-A), as done in Ref. [16] in order to reduce flow diversion by spanning the whole three main channels. Additionally, the PFOW Round One Development Sites (purple enclosed areas in Fig. 3-A) have been considered too, those are the sites for commercial renewable energy development with lease agreements granted by The Crown Estate in 2010 [55]. Since the turbines are sub-grid scale objects, a number of turbines are then allocated to all model elements that are within the areas of search, with a capacity factor > 40% and a depth > 27.5 m (see Fig. 3 panel A and B, respectively). As shown in Fig. 3-B, for the deeper (navigation) channels there is significant clearance above the turbines (water depth > 50 m). In Fig. 3, the elements surrounded by black lines indicate the array layout obtained for the Pentland Firth area following depth and capacity factor limitations. The number of turbines assigned to each model element is then the maximum number of turbines that can be allocated considering the size of the element and the spacing limits between turbines. As shown in Fig. 3-C, the number of turbines assigned to each model element are usually in the range [15–25] and the total number of turbines allocated is ≈ 2800.

3. Results

3.1. Estimates of power available for electricity generation

The available power for electricity generation at any instant in time is the work done by the thrust force per unit of time, and can be calculated as:

$$P(i,t) = \frac{1}{2}\rho A N(i) C_T(i,t) \overline{|\mathbf{u}(i,t)|}_T^3 \quad (6)$$

$$\overline{|\mathbf{u}(i,t)|}_T = \sum_{k=1}^{k=n} K_\sigma(i,k)|\mathbf{u}(i,k,t)|$$

where $\overline{|\mathbf{u}(i,t)|}_T$ is the weighted average of the velocities over the diameter of the tidal turbine. The estimates were first obtained from a 30-day SSM model run forced by tides only. For the Pentland Firth tidal turbines array (see Fig. 3) an additional sensitivity analysis was performed to show the influence of (1) tidal energy extraction feedbacks on the flow, (2) the different tidal constituents and (3) the constant or variable thrust coefficient.

The power resource from the Pentland Firth estimated without including any feedbacks of tidal energy extraction on the flow is shown in Fig. 4. From a 30-day SSM model run forced by the M_2 constituent, the theoretical resource is here defined as the power calculated from eq. (6) with $C_T = 1$, i.e. all the kinetic energy from the flow is transferred to the tidal turbines. Fig. 4 (top panel) shows that the theoretical resource is 3.52 GW on average over 30 days. A more realistic estimate can be done assuming a thrust coefficient equal to 0.85, which leads to a proportional reduction of the available average power (2.99 GW). However, a variable thrust coefficient would better reproduce the operation of a turbine with a prescribed cut-in, cut-out and rated speed, as described in Sec. 2.2, and it allows the so-called practical resource (from eq. (6) with speed dependent C_T, for values see Ref. [51] to be calculated. For the specific Pentland Firth tidal array scenario described in this work, considering just the M_2 tidal forcing and without including the momentum sink due to tidal energy extraction, the average practical resource is 2.32 GW. The practical resource is less than the theoretical resource due to the effect of the rated and cut-out speed limits (2.5 m/s and 4 m/s, for this generic turbine design). Indeed, if the flow speed is higher than the rated speed the turbine will continue to generate a constant power, as if the flow speed were equal to the rated speed. Moreover, if the flow speed exceeds the cut-out speed, the generated power is zero. From a 30-day SSM model run forced by 8 tidal constituents (M_2, S_2, N_2, K_2, K_1, O_1, P_1, Q_1), still without including any feedbacks of tidal energy extraction on the flow, Fig. 4 (bottom panel) shows that the theoretical resource is on average 4.14 GW, with an evident spring-neap cycle. However, when considering the practical resource, the variable thrust coefficient leads to a reduction of the power available for electricity generation, and this is particularly evident during the spring peaks. As a consequence the average practical resource (2.15 GW) is almost half of the average theoretical one.

When adding the feedbacks of tidal energy extraction on the flow (Fig. 5), the above considerations regarding the comparison between theoretical and practical resource are still valid. Indeed, both the M_2 only (top panel, Fig. 5) and 8 tidal constituents (bottom panel, Fig. 5) runs show a reduction of the power resource when considering a variable thrust coefficient. However, this reduction is less evident than in the undisturbed flow run. This can be explained by the tidal energy extraction itself already leading to a reduction in the flow velocities, making the influence of the variable thrust coefficient less effective. When considering the theoretical resource, the effect of the additional tidal constituents is still important (theoretical estimate is on average 1.94 GW for the M_2 only and 2.24 GW when considering all the tidal constituents). However, when the average practical resource is considered, the power resource on average for both the M_2-only estimate and 8 tidal constituents is roughly the same (1.65 GW for M_2, 1.63 GW for

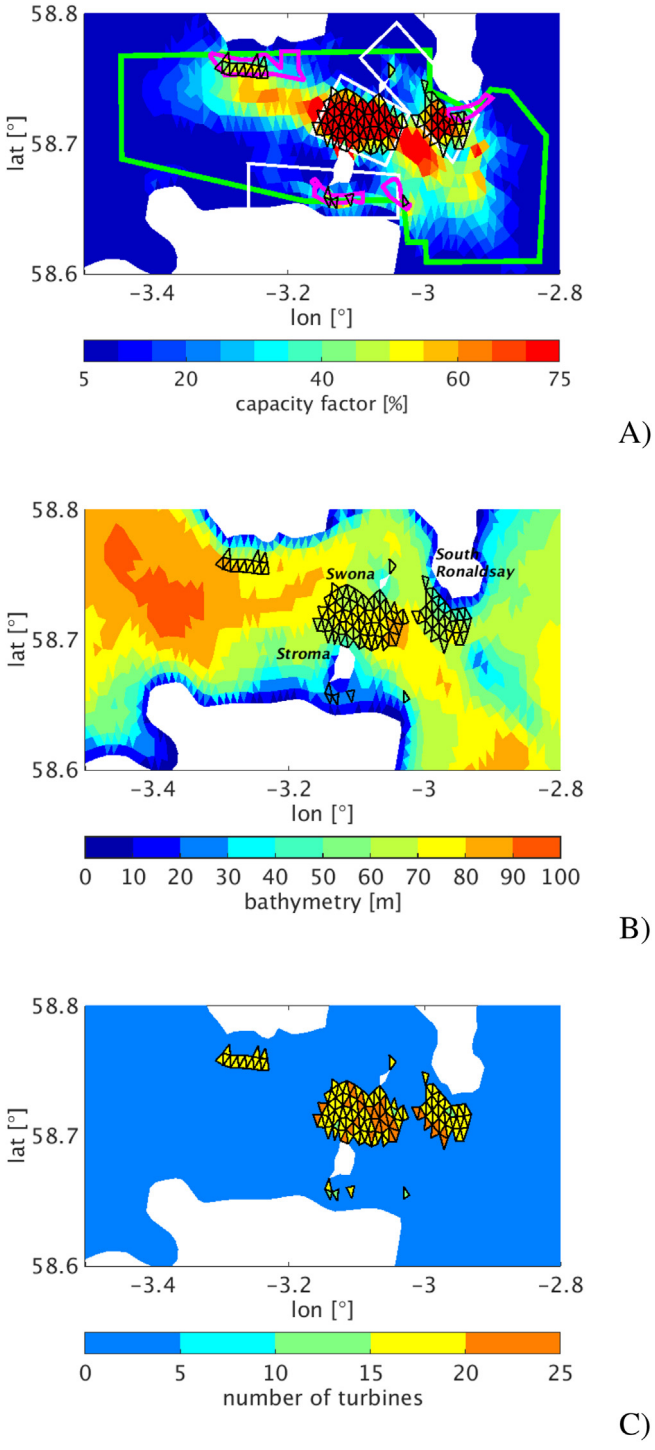

Fig. 3. Capacity factor (panel A), bathymetry (panel B) and number of turbines allocated (panel C) in the Pentland Firth. Black contoured elements are those occupied by tidal turbines. In panel A green lines indicate the area available for exploitation; purple lines delimitate the Round One Development Sites and white lines show the three areas across the channel identified for turbines placement. (For interpretation of the references to colour in this figure legend, the reader is referred to the web version of this article.)

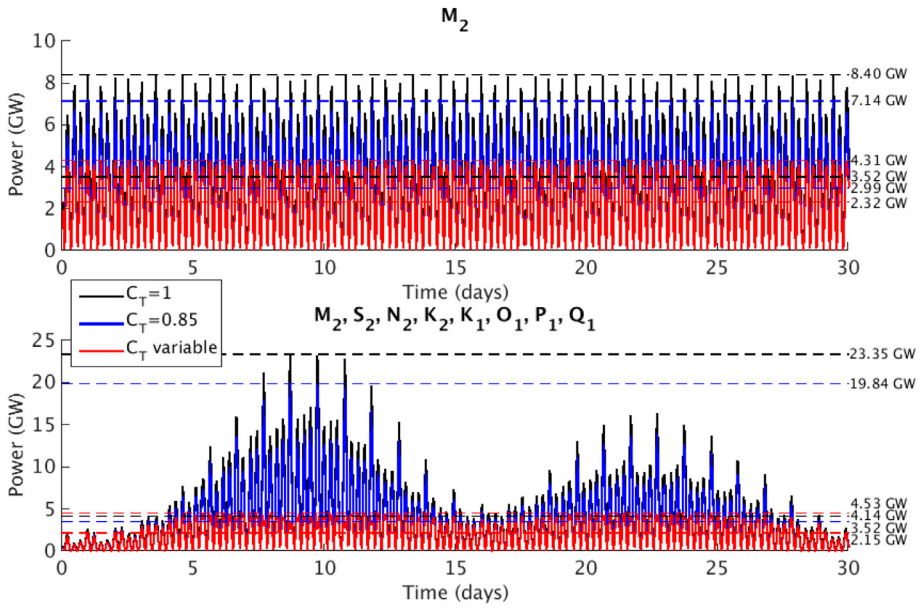

Fig. 4. Undisturbed (not including the feedbacks of tidal stream energy extraction on the flow) power resource from a tidal array in the Pentland Firth area (see Fig. 3) from a SSM run forced by (i) top panel - M_2 only and (ii) bottom panel - by 8 tidal constituents (M_2, S_2, N_2, K_2, K_1, O_1, P_1, Q_1). Sensitivity to constant (0.85 and 1) and variable thrust coefficient is shown, horizontal lines indicate the maximum and average power.

the 8 tidal constituent run). Ref. [16] found estimates of the same order of magnitude, although slightly higher. Indeed, they showed that the available power of an M_2 cycle reaches a plateau around 1.53 GW with turbines occupying the bottom part of the water column and variable thrust coefficient as in this work, but with different array layouts.

We can conclude that a more realistic estimate of the available power for electricity generation from the Pentland Firth is that obtained when including energy extraction feedbacks, 8 tidal constituents and using a variable thrust coefficient. This scenario is depicted in Fig. 5 (bottom panel, red line), which gives an average practical resource of 1.63 GW, with a maximum peak power of 4.17 GW. A final estimate of the practical power resource was obtained from the climatological year SSM model run, which includes the wind and density driven ocean circulation components. Considering tidal stream energy extraction feedbacks on the flow and using a variable thrust coefficient, the annual average power available for electricity generation is 1.64 GW. This shows that tidal currents are the principal components of the total incoming ocean currents through the Pentland Firth.

3.2. Impact of tidal energy extraction on tides

The SSM model was run for a climatological year to reproduce

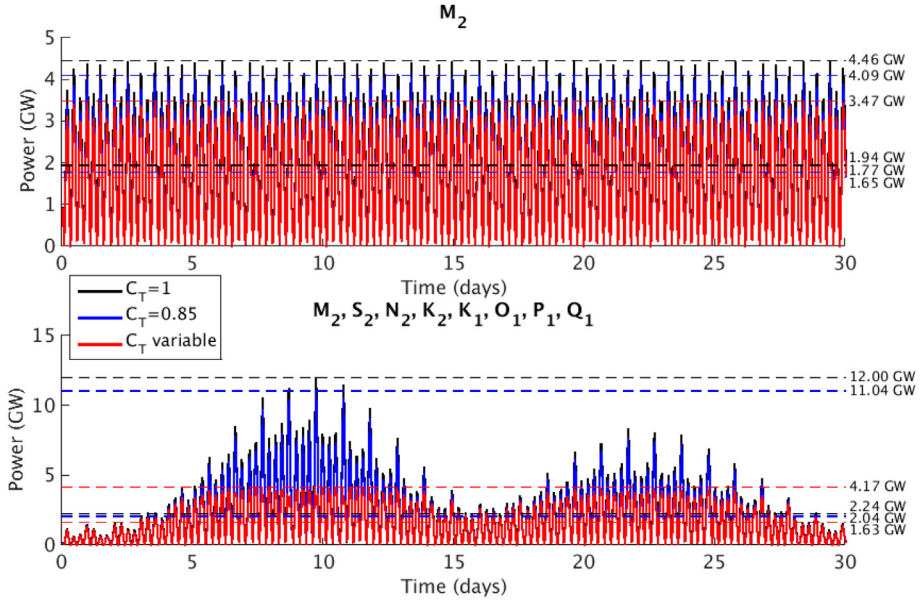

Fig. 5. Disturbed (including the feedbacks of tidal stream energy extraction on the flow) power resource from a tidal array in the Pentland Firth area (see Fig. 3) from a SSM run forced by (i) top panel - M_2 only and (ii) bottom panel - by 8 tidal constituents (M_2, S_2, N_2, K_2, K_1, O_1, P_1, Q_1). Sensitivity to constant (0.85 and 1) and variable thrust coefficient is shown, horizontal lines indicate the maximum and average power.

the baseline conditions and a tidal harmonic analysis was performed to obtain the M_2 and S_2 amplitude and phase, for both currents and elevation. The semi-diurnal constituents (in particular M_2 and S_2) are the dominant ones across the NW European Shelf. Fig. 6-A and 7-A show the baseline M_2 elevation amplitude and phase obtained by the SSM model, which reproduces the well known tidal dynamics on the NW European Shelf. The Atlantic semidiurnal Kelvin wave travels from south to north. Energy is transmitted across the shelf edge into the Celtic Sea between France and southern Ireland [56]. This wave then propagates into the English Channel where some energy propagates into the southern North Sea, the Irish Sea and the Bristol Channel, where the highest tidal elevations are observed (see Fig. 6-A, for locations see Fig. 1-A). The Atlantic wave progresses northwards, taking 5 h to travel from the Celtic sea to the north of Scotland (see Fig. 7-A). The semidiurnal wave is partly diffracted around the north of Scotland, where it turns east and travels southward along the east coast of Scotland into the North Sea [57].

This Section presents the changes in tidal dynamics due to the 1.64 GW power extraction in the Pentland Firth, where the tidal stream turbine array of Fig. 3 has been represented in the model using the approach described in Section 2.2. As far as far-field effects are concerned, Fig. 6-C shows a reduction in M_2 elevation amplitude along the east coast of UK, that can reach 1 cm. The whole North Sea is affected by an M_2 elevation amplitude decrease, which is much less than 1%, except in the vicinity of the amphidromic points (Fig. 6-E). This decrease is generated by the energy dissipation through the tidal stream turbines of the incoming Atlantic wave traveling through the Pentland Firth. An increase in M_2 tidal elevation is instead observed upstream of the Pentland

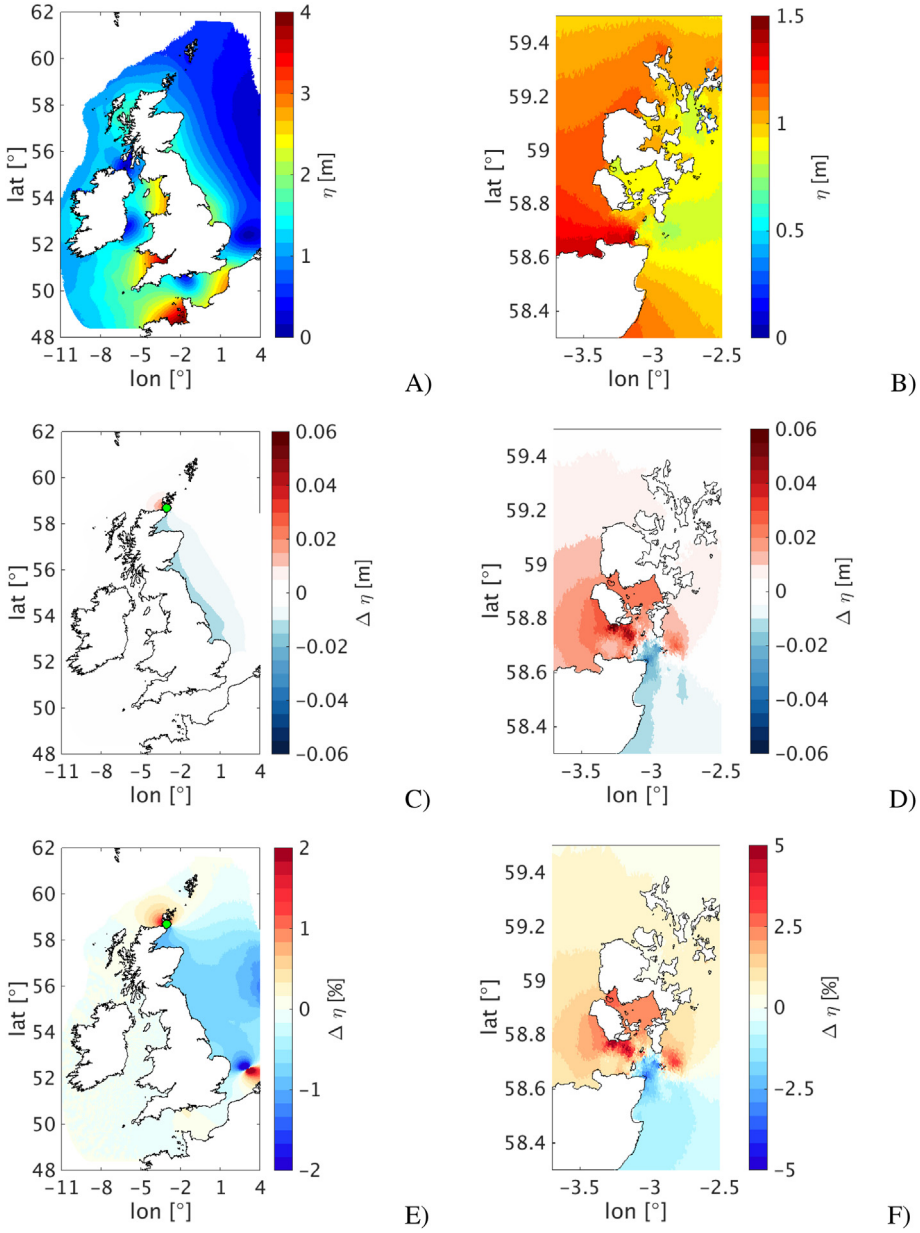

Fig. 6. Baseline (no extraction) and change in M_2 elevation amplitude due to tidal stream energy extraction in the Pentland Firth: region-wide (A) and PFOW (B) baseline; far-field (C) and near-field (D) differences; far-field (E) and near-field (F) percentage differences. Blue (red) colour represents the decrease (increase): differences are perturbed run minus baseline. The green dots in panels C and E indicate the approximate location of the tidal stream array. (For interpretation of the references to colour in this figure legend, the reader is referred to the web version of this article.)

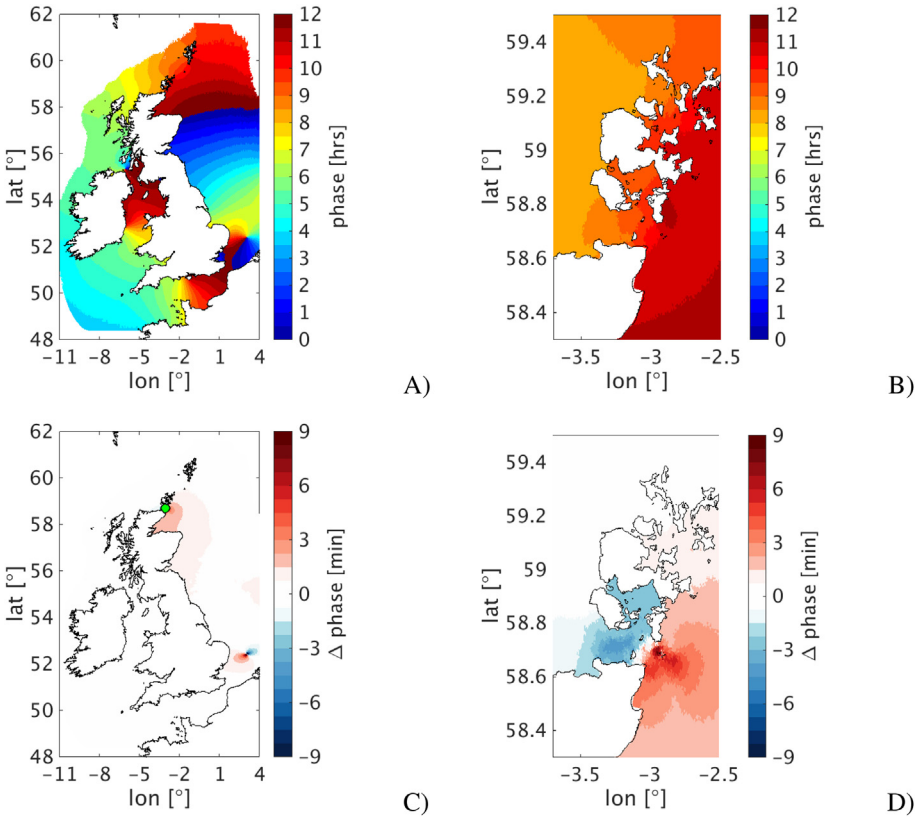

Fig. 7. Baseline (no extraction) and change in M_2 phase due to tidal stream energy extraction in the Pentland Firth: region-wide (A) and PFOW (B) baseline; far-field (C) and near-field (D) differences. Blue (red) colour represents the decrease (increase): differences are perturbed run minus baseline. The green dot in panels C indicates the approximate location of the tidal stream array. (For interpretation of the references to colour in this figure legend, the reader is referred to the web version of this article.)

Firth, which is possibly generated by blockage of flow and by a consequent decrease of kinetic energy, which is transformed into potential energy upstream of the tidal array. A similar increase/decrease pattern has been found by Ref. [17]. Near-field effects present more marked differences, with an M_2 elevation increase of up to 6 cm and a decrease that can reach 4 cm (Fig. 6-D), which corresponds to a 5% increase or decrease (Fig. 6-F).

The 1.64 GW energy extraction also affects the M_2 phase, as shown in Fig. 7-C. The semi-diurnal tidal wave is retarded by a few minutes (1–3 min) after being affected by tidal energy extraction in the Pentland Firth, while there is a small decrease in phase upstream of the Pentland Firth. The amphidromic point, located close to the Dover Strait, also shows a perturbation in the M_2 phase, with a dipole shape increase/decrease, which is certainly due to a shift in space of the amphidrome location. The M_2 phase near-field changes (Fig. 7-D) show that high water can happen up to 10 min later in the proximity of the tidal array, while the decrease in M_2 phase does not exceed 5 min.

A meaningful measure of change, when thinking about coastal management, is the change in the mean spring tidal range, indicating the mean tidal range during spring high and low water and thus taking into account also the influence of the S_2 tidal constituent (mean spring tidal range is defined as twice the sum of the M_2 and S_2 amplitudes, $H = 2\,(\eta_{M_2} + \eta_{S_2})$). Far-field changes show an increase between 1 and 3 cm along the northern Scottish mainland coast west of the Pentland Firth and in Orkney Waters (Fig. 8-C). A decrease of 2 cm is shown along all the UK east coast, reaching up to 3 cm in a localised area (Fig. 8-C). The latter corresponds to less than 1% decrease, which affects the whole North Sea (Fig. 8-E), as already observed for the M_2 elevation. Those changes are thus counteracting to some extent the sea level rise signal at high waters due to climate change [58]. Zooming into the Pentland Firth (Fig. 8-D), a wide area is affected by an increase of 5–7 cm, reaching up to 18 cm in a localised area (2 km of coast affected), while a smaller area is affected by a decrease of mean spring tidal range (no more than 10 cm). The more extreme changes correspond to 5% of the unperturbed mean spring tidal range, as shown in Fig. 8-F.

The extraction of 1.64 GW of tidal energy leads to a reduction of mean spring currents (defined as the sum of the M_2 and S_2 semi-major axis amplitudes) of the order of 1 cm/s (Fig. 9-C) along the east coast of Scotland, limited to the Moray Firth (for location see Fig. 1-A), and west of the Pentland Firth. In terms of percentage changes (Fig. 9-E), the decrease in velocity is larger downstream of the Pentland Firth, showing an 8% decrease in the undisturbed mean spring currents. There is an increase in the mean spring currents north of the Islands of Orkney (Fig. 9-C), due to the blockage of flow into the Pentland Firth and consequent diversion into northern Orkney Waters. The Pentland Firth area is affected by a larger reduction in mean spring currents, of the order 0.5 m/s, with localised increases (up to 0.24 m/s) of velocities where the flow is not blocked by tidal stream turbines (Fig. 9-D). Those large changes represent an increase or decrease of more than 15% of the undisturbed mean spring currents limited to a small spatial area (Fig. 9-F). Benthic communities may be affected by changes in current speeds [59]. However, the composition of benthic communities is stable over an approximate 1 m/s range of velocities in high velocity flow environments [59] and the effect of tidal energy extraction on benthos would be minimal.

3.3. Impact of tidal energy extraction on stratification

Here we focus on the mechanism by which tidal energy

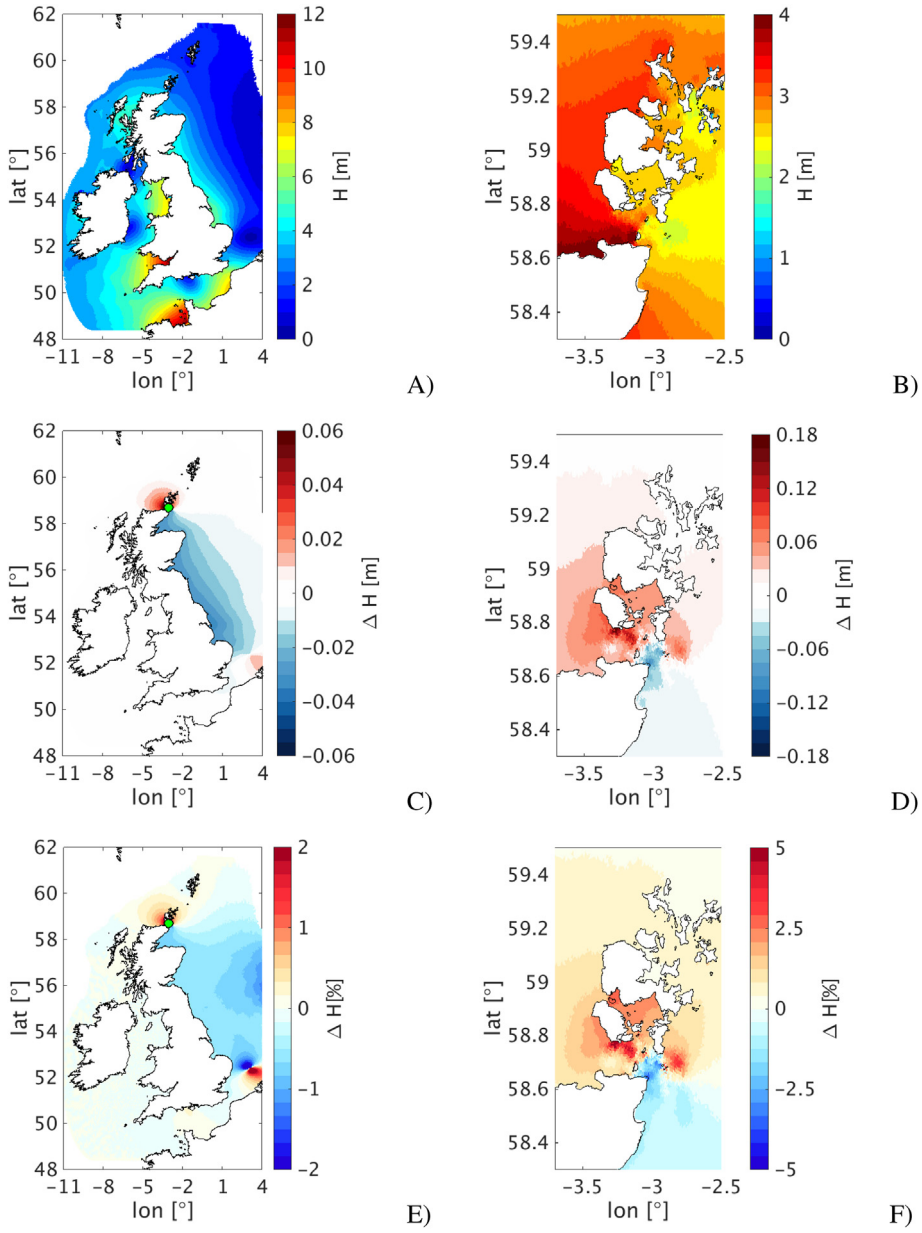

Fig. 8. Baseline (no extraction) and change in spring peak tidal range due to tidal stream energy extraction in the Pentland Firth: region-wide (A) and PFOW (B) baseline; far-field (C) and near-field (D) differences; far-field (E) and near-field (F) percentage differences. Blue (red) colour represents the decrease (increase): differences are perturbed run minus baseline. The green dots in panels C and E indicate the approximate location of the tidal stream array. (For interpretation of the references to colour in this figure legend, the reader is referred to the web version of this article.)

extraction can affect temperature, salinity and stratification on the NW European Shelf, where the spatial distribution of temperature is to a large extent determined by vertical mixing processes on the water column and tides provide the most energetic process for transport and mixing [60]. As in many shelf seas, seasonal thermal stratification occurs in the NW European Shelf when summer heating is sufficient to overcome the local mixing processes.

Features of particular importance in tidally active seas are the seasonal thermal stratification and the formation of tidal mixing fronts [61–64], which separate the seasonally stratified from permanently well-mixed or sporadically stratified waters. Tidal mixing fronts are pelagic biodiversity and productivity hotspots because they tend to separate nutrient depleted from nutrient rich waters and cross frontal exchange processes can result in enhanced concentration of nutrients and plankton. The existence of seasonal stratification is thus one of the drivers of physical, biogeochemical and biological properties in shelf-sea regions [65–67].

As shown in Section 3.2, an array of tidal stream turbines can change tidal dynamics, reduce overall tidal velocities and as a consequence decrease the energy available for tidal mixing. To investigate the influence of large scale tidal stream developments on far-field stratification, the difference between the SSM climatological years, with and without energy extraction in the Pentland Firth, were compared and the impact on temperature, salinity and stratification were investigated. In order to look at interactions of tidal energy extraction with different hydrodynamic seasonal conditions, our results are presented in the form of seasonal averages for winter (DJF: December, January, February) and summer (JJA: June, July, August).

The seasonal stratification cycle is shown by the seasonal

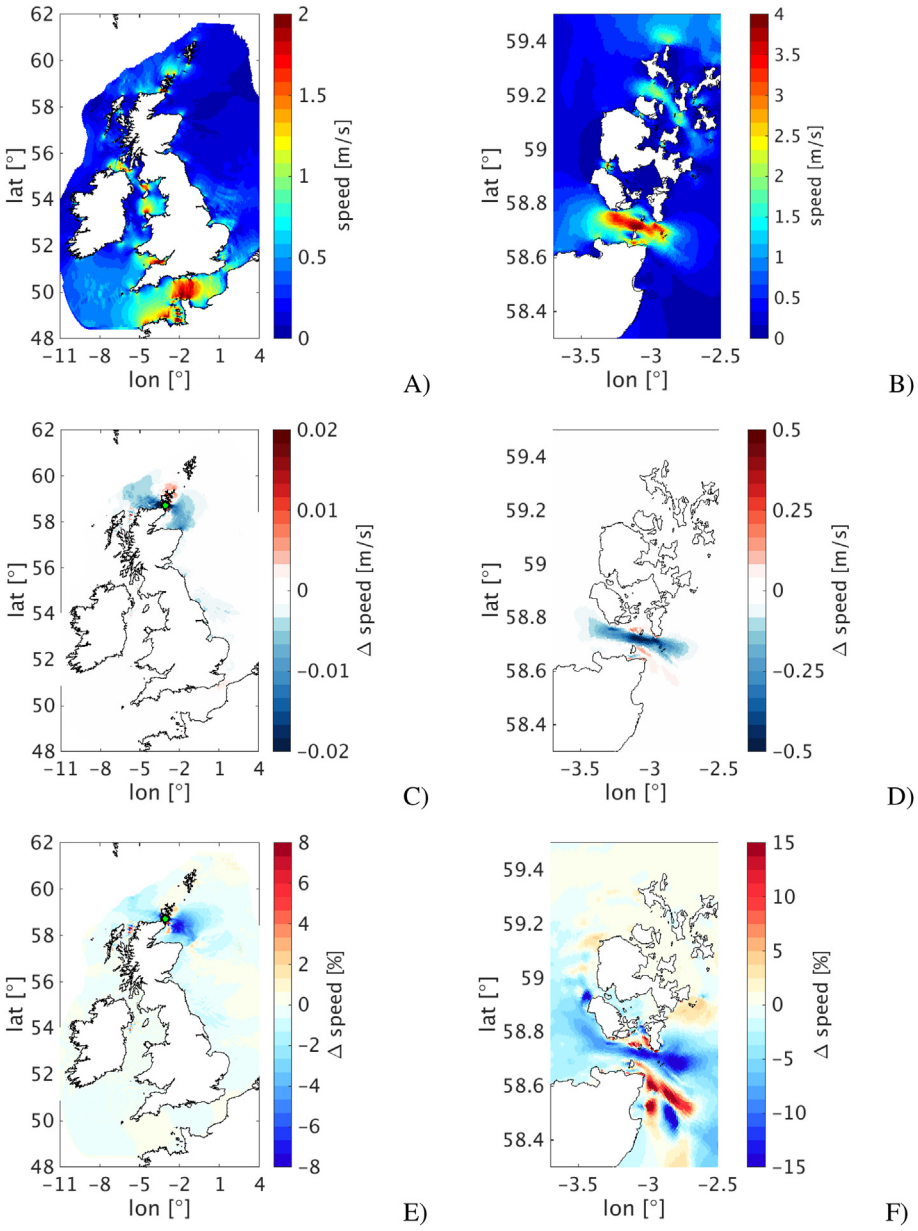

Fig. 9. Baseline (no extraction) and change in spring peak currents due to tidal stream energy extraction in the Pentland Firth: region-wide (A) and PFOW (B) baseline; far-field (C) and near-field (D) differences; far-field (E) and near-field (F) percentage differences. Blue (red) colour represents the decrease (increase): differences are perturbed run minus baseline. The green dots in panels C and E indicate the approximate location of the tidal stream array. (For interpretation of the references to colour in this figure legend, the reader is referred to the web version of this article.)

averages of the baseline Sea Surface Temperature (SST) (see Fig. 10-A and -B) and the Sea Bottom Temperature (SBT) (Fig. 11-A and -B). During winter, well-mixed conditions mean there are no differences between SST and SBT (see Fig. 10-A and 11-A). During summer, the surface layer warms rapidly under increased heat flux (see Fig. 10-B), while the lower layer remains close to winter temperatures in seasonally stratified locations. Indeed, as shown in Fig. 11-B, there is a drop in SBT in the north east region suggesting that the water there is stratified.

The difference between the perturbed and baseline SST seasonal conditions are shown in Fig. 10-C and -D. It is possible to observe that changes are smaller during winter than summer, showing a small SST increase/decrease ($< 0.15°C$) in the open sea east of Scotland and some localised areas along the west coast of Scotland (in the Firth of Clyde and south-east of Ireland, for locations see Fig. 1-A). During summer, the SST increase is much more evident and broader, extending along much of the east coast of the UK, with changes between 0.1 and 0.2°C. Those changes correspond to less than 1% increase, only in a few small areas does it reach up to 2% (see Fig. 10-F). Fig. 11-C and -D show the anomalies on SBT generated by tidal energy extraction in the Pentland Firth: during winter we can identify the same changes already seen in winter SST, while in summer the distinctive feature is a decrease of bottom temperature along the east coast of the UK, that can exceed 0.3°C. In Fig. 11-F, we can observe a 1% decrease of SBT along all east coast of UK, with a distinctive feature in the open sea east of the Moray Firth, showing a decrease higher than 3% of the unperturbed SBT. The 1.64 GW extraction in the Pentland Firth thus affects the SBT more than SST, producing a larger decrease in SBT than the increase in SST.

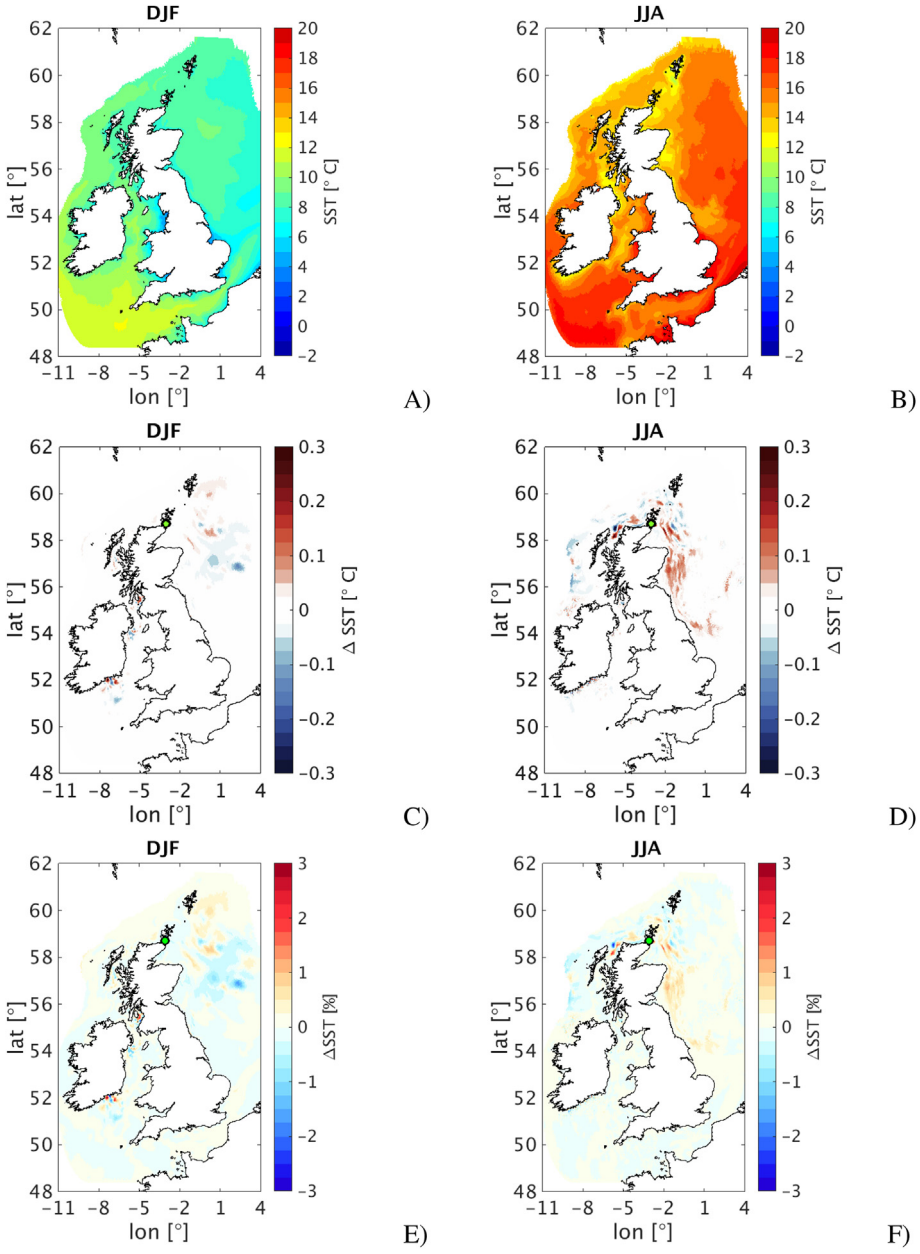

Fig. 10. Seasonal baseline (no extraction) and change in Sea Surface Temperature (SST) due to tidal stream energy extraction in the Pentland Firth: winter - DJF (A) and summer - JJA (B) region-wide baseline; winter (C) and summer (D) far-field differences; winter (E) and summer (F) far-field percentage differences. Blue (red) colour represents the decrease (increase): differences are perturbed run minus baseline. The green dots indicate the approximate location of the tidal stream array. (For interpretation of the references to colour in this figure legend, the reader is referred to the web version of this article.)

Percentage changes in horizontal transport generated by tidal energy extraction are described in Sec. 3.5. Whilst changes to horizontal transport may contribute to the temperature modifications, we believe the main contribution is the change in vertical mixing. In seasonally stratified seas, the seasonal and spatial distribution of stratification can be measured through the potential energy anomaly (PEA) defined as:

$$PEA = -\frac{1}{h}\int_{-h}^{0} gz\Big(\rho(T,S) - \overline{\rho}\Big(\overline{T},\overline{S}\Big)\Big)dz \tag{7}$$

where h is the water depth, g is the gravitational acceleration, ρ is the density, T is the temperature, S is the salinity, the overbar indicates a mean average over the same depth as the integration [63]. The physical interpretation of this metric is the potential energy (per unit depth) required to fully mix the water column. Where PEA is equal to zero there is a fully mixed water column and, for convenience, PEA is defined to be positive for stable stratification. Shelf waters are well mixed in winter, while during spring-summer the water column stratification onset is caused by decreased wind stress and freshwater inputs and increased summer-time heat flux [61].

Fig. 12-A and -B show the PEA baseline for winter and summer, with the 10 J/m^2 delimiting the extent of the stratified regions. During winter, water is mixed over the entire shelf, apart from a localised area along the west coast of Scotland (Firth of Clyde), due

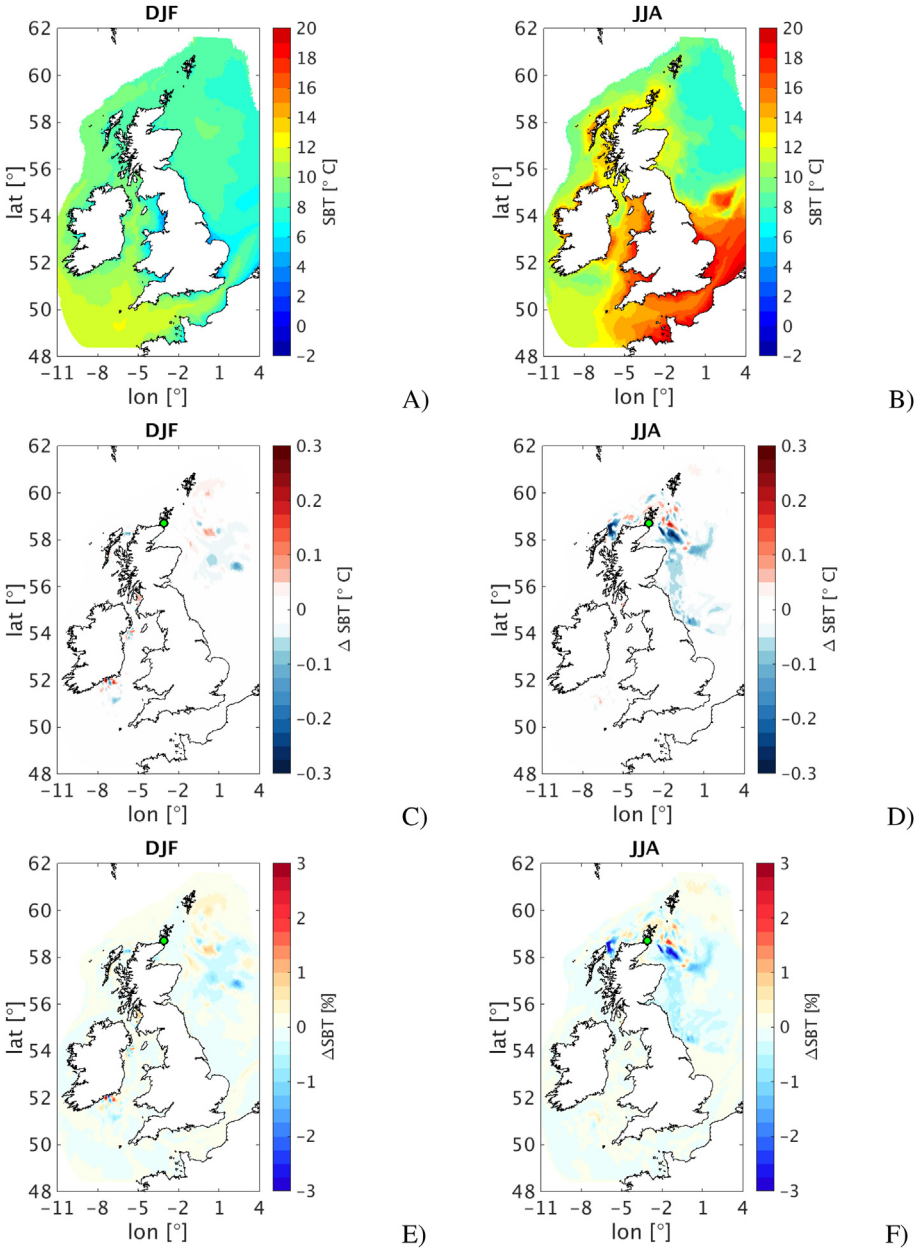

Fig. 11. Seasonal baseline (no extraction) and change in Sea Bottom Temperature (SBT) due to tidal stream energy extraction in the Pentland Firth: winter - DJF (A) and summer - JJA (B) region-wide baseline; winter (C) and summer (D) far-field differences; winter (E) and summer (F) far-field percentage differences. Blue (red) colour represents the decrease (increase): differences are perturbed run minus baseline. The green dots indicate the approximate location of the tidal stream array. (For interpretation of the references to colour in this figure legend, the reader is referred to the web version of this article.)

to the effect of riverine discharges. During summer, the extent of mixed waters decreases, with the 10 J/m^2 contour (Fig. 12-B), separating the stratified waters from the mixed one, in agreement with the position of tidal mixing fronts identified by Ref. [62] and with the summer distribution of observed thermal fronts found by Ref. [68]. The action of tidal energy extraction does not have any influence on mixed waters. Indeed, as shown in Fig. 12-C, small changes in PEA are identifiable only in small areas that were stratified, while no perturbations are observable elsewhere. During summer (Fig. 12-D) there is an evident increase in PEA, telling us that if the waters are stratified, the reduction of vertical mixing due to the operations of turbines can increase water stratification, as already shown by the summer SST and SBT anomaly pattern. The extent of the stratified regions does not greatly change with tidal energy extraction, with the position of the 10 J/m^2 contour remaining unchanged. Thus the enhanced biological production and pelagic biodiversity linked to fronts should not be affected. However, where stratification does occur, its strength increases, between 1 and 2 J/m^2 over a wide area in the North Sea and exceeds 10 J/m^2 in some localised areas (Fig. 12-D), which is an increase equal to 10–20% of the baseline summer PEA (Fig. 12-F). That increase may have implications particularly when/where the stratification is weak, for example the timing and magnitude of phytoplankton blooms can be influenced by very small changes in water column stability [69].

Salinity changes have not been shown in this Section because it has been found that they do not exceed 0.1% change and PEA already takes into account its contribution. The Sea Surface Salinity

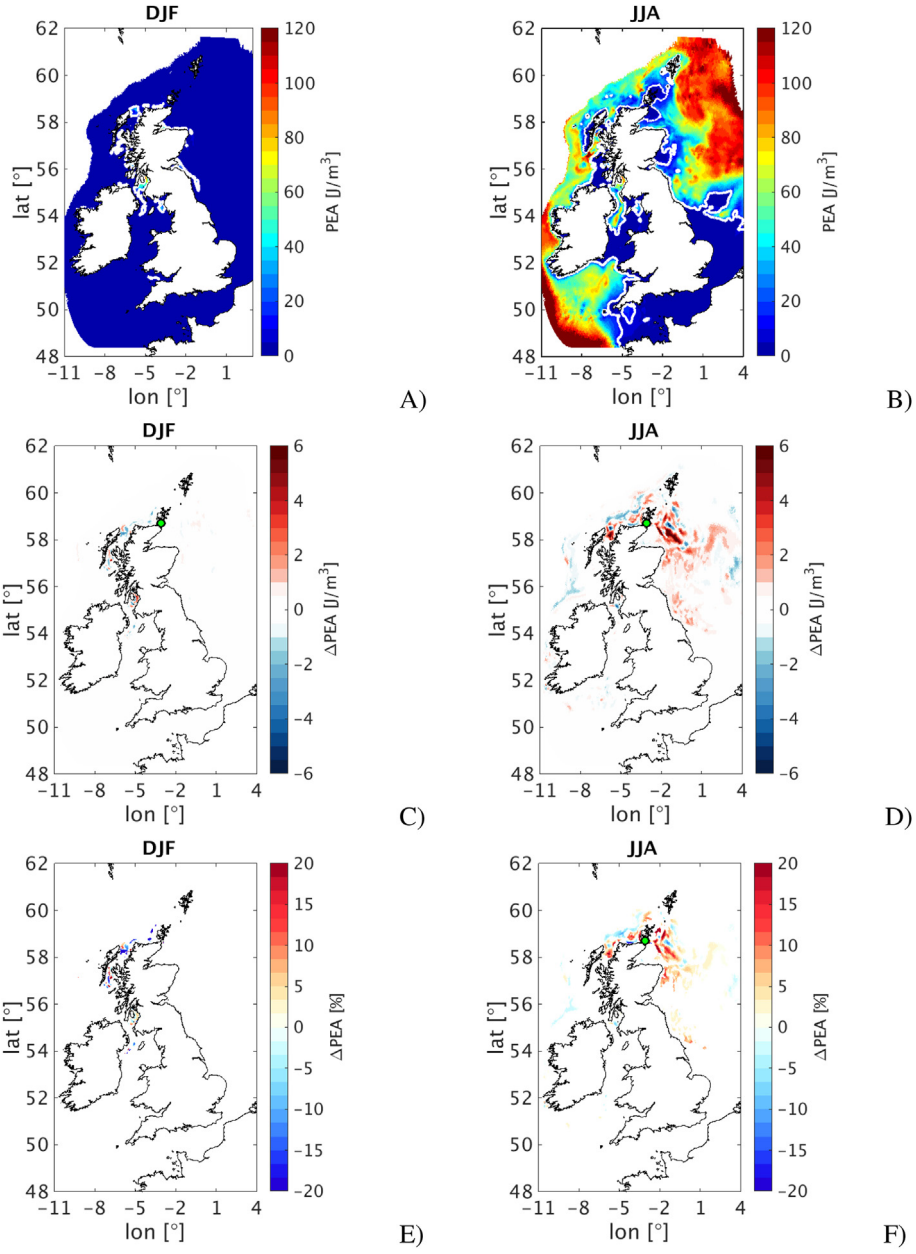

Fig. 12. Seasonal baseline (no extraction) and change in Potential Energy Anomaly (PEA) due to tidal stream energy extraction in the Pentland Firth. Winter - DJF (A) and summer - JJA (B) are the region-wide baseline conditions: the white dashed line is the 10 J/m^2 contour line separating stratified from mixed waters. Winter (C) and summer (D) are far-field differences. Winter (E) and summer (F) are far-field percentage differences: masked out for clarity percentage differences associated to absolute differences less than 1 J/m^2. Blue (red) colour represents the decrease (increase): differences are perturbed run minus baseline. The green dots indicate the approximate location of the tidal stream array. (For interpretation of the references to colour in this figure legend, the reader is referred to the web version of this article.)

(SSS) and Sea Bottom Salinity (SBS) winter anomaly patterns are similar to the winter SST/SBT ones, and in summer both SSS and SBS perturbations show the same pattern as the summer SST.

3.4. Impact of tidal energy extraction on residual currents and volume transport

Residual flows are persistent flows which remain after the periodic tidal flows have been averaged out, they have several causes, including wind and density differences (baroclinic flows). Fig. 13 shows the intensity of seasonal depth-averaged residual currents in the North Sea. The broad scale circulation patterns of Scottish waters, such as the Scottish coastal current, North Sea inflow, Slope current and Dooley current, are well reproduced [70,71]. The mean currents of the North Sea form a cyclonic circulation. The bulk of the transport in this circulation is concentrated to the northern part of the North Sea due to major water exchange with the Norwegian Sea, where the main inflow and outflow occur. A little inflow occurs through the English Channel, while considerable inflows take place east of the Shetland Islands and between Shetland and the Orkney Islands [71] (for locations see Fig. 1-A).

The installation of a large scale tidal energy array influences the residual circulation, mainly weakening the circulation within the Pentland Firth (a reduction of up to 0.2 m/s in both winter and summer, not shown). The transport across the Pentland Firth has been calculated along a section at the western entrance of the channel, it is mostly directed from west to east during winter months (0.026 Sv), while is negligible during summer. Tidal energy

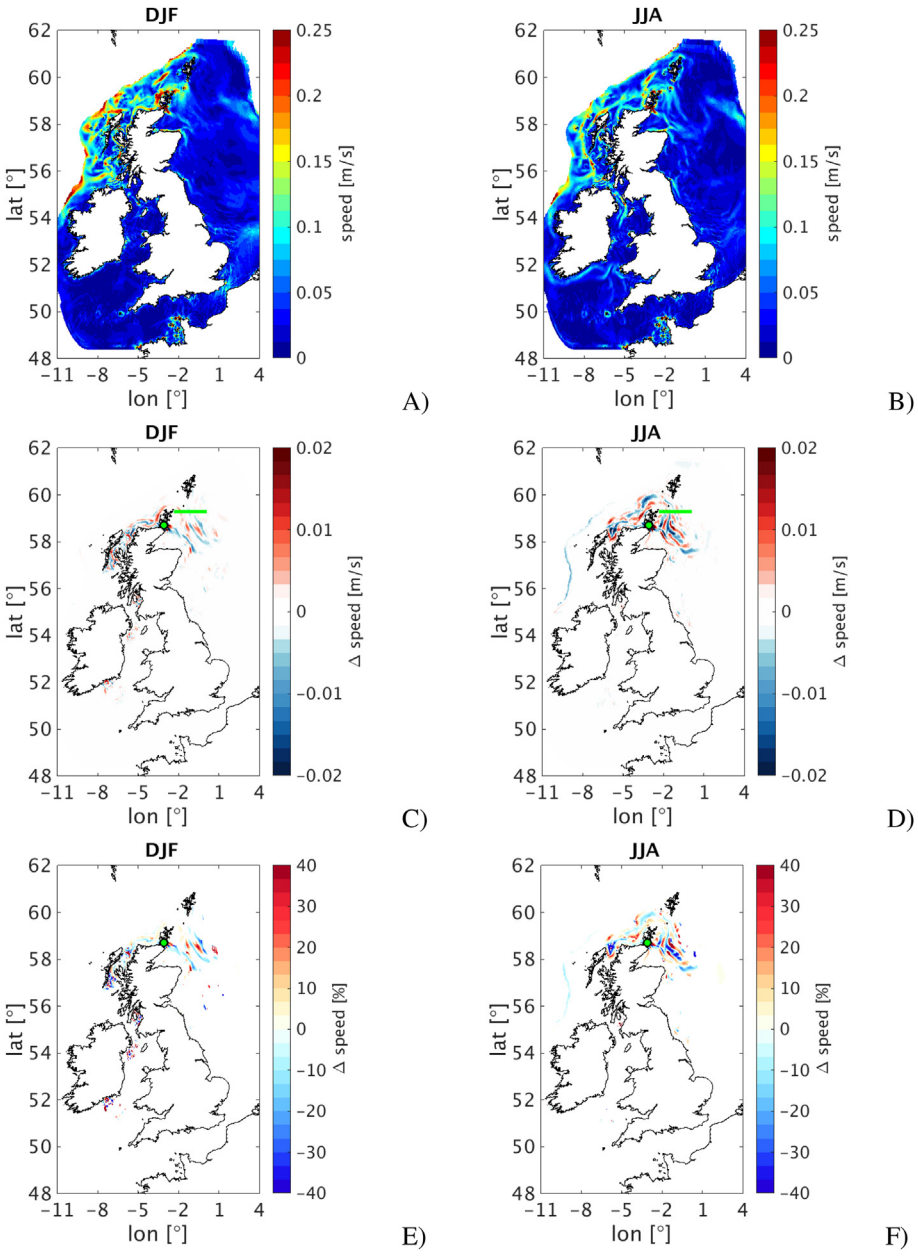

Fig. 13. Seasonal baseline (no extraction) and change in depth-averaged residual currents due to tidal stream energy extraction in the Pentland Firth: winter - DJF (A) and summer - JJA (B) region-wide baseline; winter (C) and summer (D) far-field differences; winter (E) and summer (F) far-field percentage differences: masked out for clarity percentage differences associated to absolute differences less than 0.003 m/s. Green line in panels C and D is the JONSIS - Joint North Sea Information System transect. Blue (red) colour represents the decrease (increase): differences are perturbed run minus baseline. The green dots indicate the approximate location of the tidal stream array. (For interpretation of the references to colour in this figure legend, the reader is referred to the web version of this article.)

extraction leads to a reduction, by 24%, of the inflow of the Atlantic Water into the North Sea during winter. It could also lead to a tendency to trap tracers within the Firth and/or to changes in transport pathways for suspended and dissolved materials, which are however outside the scope of this manuscript and require further studies.

As shown in Fig. 13, the effects of tidal energy extraction on residual currents are observed not only in the Pentland Firth, but are evident also between Orkney and Shetland. Changes can lead to a decrease/increase up to 0.02 m/s, which are more intense and over a wider area during summer than in winter (Fig. 13-C and -D). Those changes account for 40% of the residual water velocity in the affected region (Fig. 13-E and -F). That region is largely influenced by the Fair Isle Current (FIC) entering the North Sea between Orkney and Shetland [72]. The Fair Isle current brings North-East Atlantic water into the North Sea derived from the Slope current flowing north along the NW European Shelf edge [73]. Changes in residual currents due to tidal energy extraction can influence biological processes, as the FIC is a major transport route for fish larvae and associated with the variability of fish stock recruitment, plankton and epifauna in that area [73–75]. Volume transport with and without tidal energy extraction has been estimated through the JONSIS - Joint North Sea Information System transect (green line in Fig. 13-C and D), that captures the water originating west of Scotland and is a mixture of coastal and Atlantic water. However, a very small increase of the inflow of water into the North Sea via the FIC can be attributed to tidal energy extraction in the Pentland Firth: 0.3% during both summer and winter.

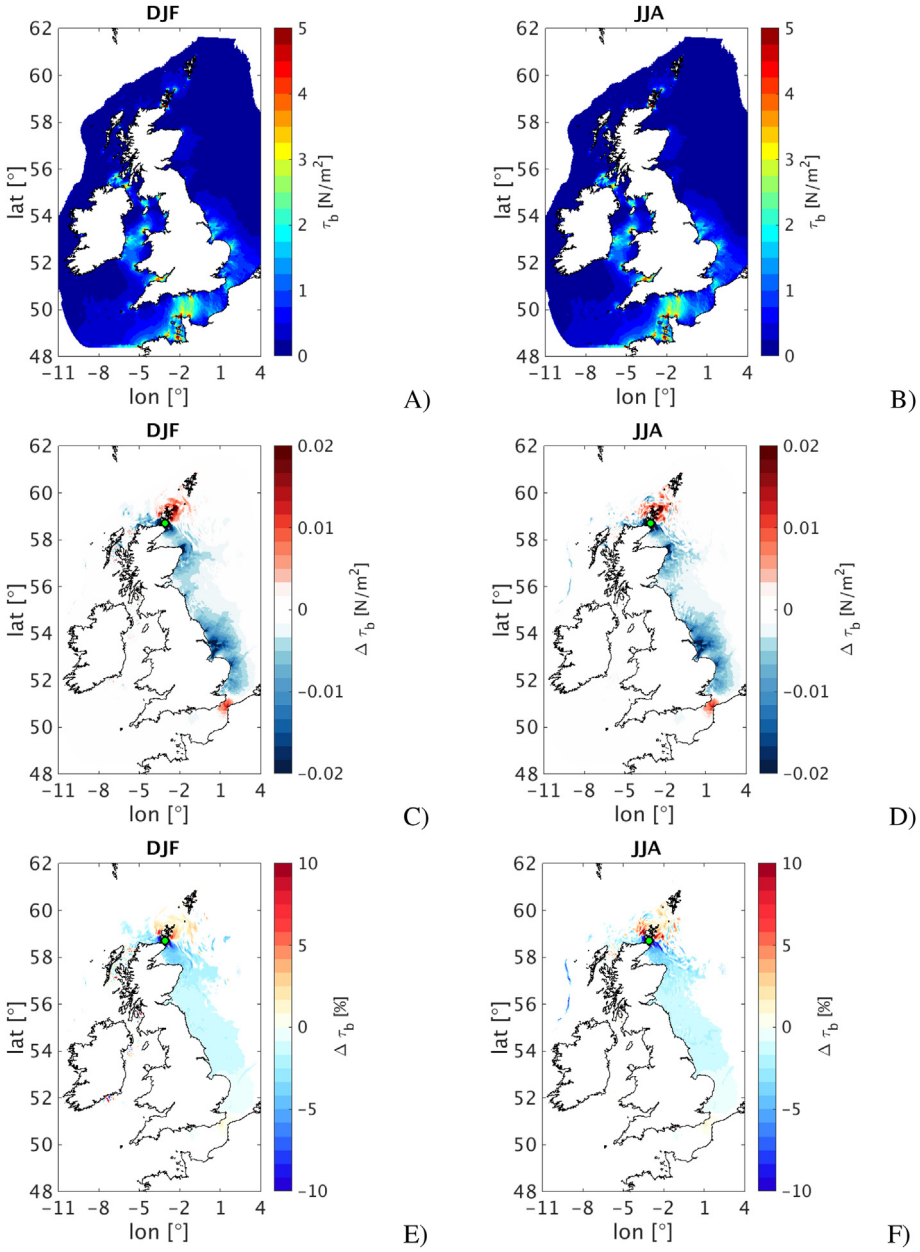

Fig. 14. Seasonal baseline (no extraction) and change in current-induced bed shear stress due to tidal stream energy extraction in the Pentland Firth: winter - DJF (A) and summer - JJA (B) region-wide baseline; winter (C) and summer (D) far-field differences; winter (E) and summer (F) far-field percentage differences: masked out for clarity percentage differences associated to absolute differences less than 0.002 N/m^2. Blue (red) colour represents the decrease (increase): differences are perturbed run minus baseline. The green dots indicate the approximate location of the tidal stream array. (For interpretation of the references to colour in this figure legend, the reader is referred to the web version of this article.)

3.5. Impact of tidal energy extraction on bed shear stress

It is possible to gain significant insight into the sediment transport regime of a region by looking at the distribution of bed shear stress, τ_b, as this is the major control on sediment deposition and erosion rates. The bed shear-stress is the frictional force exerted by the flow per unit of area of bed and it is due to both currents and waves (not considered in this work). Depending on the value of τ_b compared to the erosion/deposition critical stresses for the sediment of interest, it is possible to determine the likely locations of erosions and deposition of that sediment type [76,77]. In this work, we are interested in knowing if tidal energy extraction induced disturbance can significantly alter the bed shear stress and, consequently, erosion/deposition processes and benthic species environment.

Fig. 14-A and -B show the seasonal bed-shear stress magnitude directly provided by FVCOM as $\tau_b = \rho C_D |\mathbf{u_b}|^2$, where $\mathbf{u_b}$ is the bottom current, which include the tidal, wind and density driven components, and C_D is the drag coefficient calculated from the spatially constant roughness length across the whole model domain. Fig. 14-C and -D show both an increase in seasonally averaged current-induced bed shear stress around the Orkney Islands, while reductions in shear stress were detected in the Pentland Firth and all along the UK east coast, with the largest reduction in the vicinity of the Wash (for location see Fig. 1-A). An increase is also observed in the strait of Dover (for location see

Fig. 1-A). These results show a similar pattern to that found by Ref. [17]. No significant seasonal differences are observed.

In the Wash, where waters are shallow, mud and sand sediments are present [78] and bed shear stress is relatively large, a reduction in bed shear stress could lead to a increase in deposition rates and a decrease in surface particulate matter. Further studies are required to assess if the estimated reduction in bed shear stress could lead to changes in water turbidity. As suggested by Ref. [79], the 50% attenuation of current speed (for mud sediments) could produce detectable decreases of water column turbidity, which can then in turn increase light penetration and lead to higher primary productivity in the area.

In Orkney waters, the increase in bed shear stress has to be assessed against the background natural seabed disturbance. The area is characterised by bedrock and coarse sediments (BGS UK Continental Shelf Seabed Sediments, available through OneGeology portal) and the maximum bed shear stress can reach 25 N/m^2 (not shown). Although changes in bed shear stress can exceed 10%, this increase would not affect the erosion of coarse sediments. There are however a few sand banks in the Pentand Firth [18,80] which could be altered by the bed shear stress changes detected in this work. For smaller scale tidal stream turbines arrays, impacts on sediment transport in the region have been already performed by Refs. [18] and [19]. Our results suggest that it would be of interest to extend those works to include a larger scale tidal stream turbine array and to study the impacts not only in the Pentland Firth, but also in the northern Orkney Islands.

4. Discussion

The energy security for future generations can potentially achieve a significant contribution from the energy available in high tidal velocity environments, such as in the Pentland Firth. This area, on which this work has been focused, is where one of the world's first large-scale arrays is likely to be located, with tidal turbines already placed for testing purposes in real sea conditions. While the commercial development of the technology is at an early stage, the scientific community can help in boosting the tidal stream energy sector by understanding two possible outstanding factors impeding its commercialization: (1) the economical one linked to the power that can be realistically made available for electricity generation and (2) the possible impacts on marine hydrodynamics and consequently on the marine ecosystem and mobile marine species behaviour.

An estimate of the available power for electricity generation from the Pentland Firth is 1.64 GW, which requires thousands of turbines to be deployed. The latter was obtained considering the reduction in the resource by the energy extraction itself and a realistic representation of the tidal turbine operations. That estimate includes also the wind- and density-driven components of the ocean current, although these contributions have been shown to be negligible in this high tidal velocity environment. It is worth comparing this figure with the yearly average instantaneous UK electricity demand of 34.55 GW [81], showing that the Pentland Firth can potentially provide 5% of the UK demand. This gives us the order of magnitude of the Pentland Firth potential. Although we included more tidal constituents, our estimate is of the same order of magnitude as was found by Ref. [16]: 1.53 GW average over an M_2 cycle. However, some power will be lost during the electricity generation process and more or less energy could be potentially generated by using other types of devices and/or different array layouts. For example, if different rotor swept areas or thrust coefficient values are applied, the model will predict slightly different power levels. Whilst the applied methodology is valid and the generic tidal turbine parameters used are sufficiently realistic as to be acceptable to stakeholders [51], more or less energy could be potentially generated by other types of devices, whose power curves should be made available by the industry for future tidal stream energy sites. Additionally, our findings are based on a specific scenario with generic turbines deployed in this arrangement close to the bed and located in locations that meet three conditions: (i) a minimum water depth to have the turbines underwater in all tidal stages, (ii) a minimum turbine spacing to eliminate wake effects and (iii) a minimum capacity factor [52] to place the turbines in locations that are economically viable. A different layout may well yield a different result. It also has to be noted that the SSM model resolution does not allow small scale (< 1 km) interactions between turbine wakes to be reproduced and optimisation techniques to be applied for the positioning and individual tuning of turbines, that could potentially increase the extracted energy [82].

It was found that the very large scale tidal stream array can introduce noticeable far-field changes on tidal elevation, showing a decrease in tidal elevation along the whole east coast of the UK. This is caused by the energy dissipation of the incoming Atlantic wave travelling through the tidal stream turbines in the Pentland Firth. The decrease along the coast in terms of mean spring tidal range is 2 cm (up to 3 cm in the Wash), while an increase, of the same order of magnitude, affects a much smaller area upstream of the Pentland Firth. Generalizing, we can conclude that, in the far-field, tidal elevation mainly increases upstream of the tidal array location (considering the direction of propagation of the tidal wave), and that tidal elevation decreases downstream, this is has also been shown by Ref. [17] for the Pentland Firth impacts study and by Refs. [30] and [28] for the Minas Passage (Canada). Those, at the time of writing, are the only studies available on very far-field effects. The modelled decrease in tidal elevation along the east coast of the UK can counteract to some extent the sea level rise signal at high waters due to climate change [58]. However, in the near-field of the tidal farm the increase of 5–7 cm is the dominant effect (up to 18 cm in a very localised area).

Extracting 1.64 GW of energy from the ocean changes marine current patterns, of both tidal and residual flows, which can be slowed down by the turbines action or intensified due to flow blockage and diversion processes. On the local scale there is a reduction of the order of 0.5 m/s in mean spring currents and localised increases of velocities, due to flow diversion where it is not blocked by the turbines, as was observed by Ref. [16] for a similar amount of energy extracted. Far-field reduction of the mean spring currents is smaller than in the vicinity of the tidal farm, of the order of 1 cm/s both upstream and downstream of the Pentland Firth, while an increase is observed in the northern Orkney Waters due to the blockage of flow into the Pentland Firth. Changes in marine currents may also lead to changes in sediment dynamics and benthic communities, that should be addressed in future work. However, the effect of tidal energy extraction on benthos might be minimal, since their composition is stable over an approximate 1 m/s range of velocities in high velocity flow environments [59], which is above the range of changes we found. As far as sediments are concerned, an increase in bed shear stress has been observed around Orkney Islands and in the Strait of Dover, while reductions in bed-shear stress were detected in the Pentland Firth and all along the UK east coast, with the largest reduction in the vicinity of the Wash. Similar pattern has been observed also by Ref. [17]. Further studies are required to assess if the estimated reduction in bed shear stress could lead to changes in water turbidity, as suggested by Ref. [79]; which can in turn increase light penetration and consequently primary productivity. On the other hand, the increase in bed-shear stress around the northern Islands of Orkney highlights the need for a study investigating the possible presence and behaviour of sand-banks that could be mobilized in that area,

extending the studies of Refs. [18] and [19] to include a large scale tidal stream turbine array and to study the impacts in the Orkney Waters area. Residual currents are modified in the vicinity of the array and as away as hundreds kilometres, as found also by Ref. [29] for a tidal farm in the Celtic Sea. Additionally, we found that the changes show a seasonality, being larger during summer. A 40% change (increase or decrease) of the residual velocities can be reached between Orkney and Shetland, which is a region largely influenced by the FIC entering the North Sea. The FIC is a major route for fish larvae, plankton and epifauna and a very small increase (0.3%) in the inflow of waters into the North Sea has been found. However, changes in transport pathways of passive tracers, as suspended sediments and larvae, require further studies to be properly assessed.

As tidal stream energy extraction can overall reduce tidal velocities, and in consequence can decrease the energy of tidal mixing, the balance between stratification and vertical mixing processes in a tidally active and seasonally stratified sea, as the NW European Shelf, can be perturbed. The interaction between tidal stream energy extraction with the different seasonal hydrodynamic conditions showed region-wide impacts on the summer time temperature and PEA. During winter the action of tidal stream energy extraction does not have any detectable influence on well-mixed waters, while during summer there is an evident increase in the water column stratification. This tells us that, if the waters are stratified, the reduction of vertical mixing due to the operations of turbines can increase the strength of water stratification, thus exacerbating the predicted climate change stratification increase [60]. These longer term seasonal timescales have never been addressed in previous studies. PEA changes of the order of 10–20% are observed, which may have implications particularly when/where the stratification is weak, as a very small increase in water column stability can, for example, trigger phytoplankton blooms [69]. However, the extent of the stratified region does not greatly change, thus the enhanced biological and pelagic biodiversity hotspots, i.e. tidal mixing front locations, are not perturbed. These are areas of enhanced concentration of nutrients and plankton, due to cross-frontal exchange processes, and separate the seasonally stratified water from the permanently well-mixed waters.

The evaluation of the possible effects of the perturbed marine hydrodynamic processes on the marine ecosystem and mobile marine species behaviour is an on-going topic of research. The complex dynamics of shelf seas and the species that inhabit them, requires further understanding of the habitat selection driven by natural variables, by competition and/or predator-prey interactions of habitat use, before the potential impacts of anthropogenically induced disturbances can be evaluated. Patterns in habitat use can coincide with particular oceanographic conditions including changes in SST, frontal activity, the strength of the tidal currents [83] and enhanced primary productivity locations [84]. Future work would be required to evaluate whether the predicted changes due to tidal stream energy extraction will change the availability and location of critical habitats for marine species, and as a consequence changes in animal behaviours.

5. Conclusions

A comprehensive assessment of the tidal energy resource available for electricity generation in the Pentland Firth (Scottish Waters, UK) showed that a large theoretical array of tidal stream turbines can make available 1.64 GW on average for electricity generation, requiring thousands of turbines to be deployed. That estimate takes into account the tidal stream energy extraction feedbacks on the flow and considers the realistic operation of a generic tidal stream turbine, which is limited to operate in a range of flow velocities due to technological constraints. Our estimate is also based on using existing/near future tidal stream technology, i.e. with 20 m diameter turbines being deployed close to the bed.

The ocean response to the 1.64 GW power extraction has been numerically simulated using the SSM model, an unstructured 3D ocean model (FVCOM) which can reproduce a typical annual cycle of the NW European Shelf hydrodynamics. Tidal elevation mainly increases in the vicinity of the tidal farm, while far-field effects show a decrease in the mean spring tidal range of the order of 2 cm along the whole east coast of the UK, possibly counteracting some part of the predicted sea level rise due to climate change. Marine currents, both tidal and residual flows, are also affected. They can slow down due to the turbines' action or speed up due to flow diversion processes, on both a local and regional scale.

The ocean response to tidal stream energy extraction has been analysed not only at the temporal scale of a spring-neap tidal cycle, but also on longer term seasonal timescales, which have never been addressed in previous studies. The strongest signal in tidal velocities is an overall reduction, which can in turn decrease the energy of tidal mixing and perturb the seasonal stratification on the NW European Shelf. Although the strength of summer water stratification has been found to slightly increase, the extent of the stratified region does not greatly change, thus the tidal mixing front locations are not displaced. Such large scale tidal stream energy extraction is unlikely to occur in the near future, but such potential changes should be considered when planning future tidal energy exploitation. It is likely that further large scale developments around the NW European Shelf will interact with each other and could, for example, intensify or weaken the changes predicted here, or even be used as mitigation measures (e.g. coastal defence) for other changes (e.g. climate change).

A future extension of this study to other locations available for exploitation of tidal stream energy extraction could give a further insight into how the physical processes, highlighted here and the mechanisms behind them, are also common to other areas. Furthermore, the impacts on the marine environment should be put in the broader context of the possibly greater and global ecological threat of climate change, in order to study whether tidal energy extraction can ameliorate or exacerbate the anthropogenic disturbance of climate change on the marine system.

Acknowledgments

This work is part of the EcoWatt2050 project, funded by the Engineering and Physical Sciences Research Council (EPSRC), grant reference EP-K012851-1. The work was also supported by NOC National Capability programme in Ocean Modelling.

References

[1] A.S. Bahaj, Generating electricity from the oceans, Renew. Sustain. Energy Rev. 15 (7) (2011) 3399–3416.
[2] R. Pelc, R.M. Fujita, Renewable energy from the ocean, Mar. Policy 26 (6) (2002) 471–479.
[3] D. Magagna, A. Uihlein, Ocean energy development in Europe: current status and future perspectives, Int. J. Mar. Energy 11 (2015) 84–104.
[4] M. Lewis, S. Neill, P. Robins, M. Hashemi, Resource assessment for future generations of tidal-stream energy arrays, Energy 83 (2015) 403–415.
[5] J. Wolf, I.A. Walkington, J. Holt, R. Burrows, Environmental impacts of tidal power schemes, in: Proceedings of the Institution of Civil Engineers-maritime Engineering, vol. 162, Thomas Telford Publishing, 2009, pp. 165–177.
[6] A.B. Gill, Offshore renewable energy: ecological implications of generating electricity in the coastal zone, J. Appl. Ecol. 42 (4) (2005) 605–615.
[7] R. Inger, M.J. Attrill, S. Bearhop, A.C. Broderick, W. James Grecian, D.J. Hodgson, C. Mills, E. Sheehan, S.C. Votier, M.J. Witt, B.J. Godley, Marine renewable energy: potential benefits to biodiversity? An urgent call for research, J. Appl. Ecol. 46 (6) (2009) 1145–1153.
[8] G.W. Boehlert, A.B. Gill, Environmental and ecological effects of ocean renewable energy development: a current synthesis, Oceanography 23 (2)

(2010) 68–81.
[9] A. Copping, N. Sather, L. Hanna, J. Whiting, G. Zydlewski, G. Staines, A. Gill, I. Hutchison, A. O'Hagan, T. Simas, J. Bald, S. C, J. Wood, E. Masden, Annex IV 2016 state of the science report: environmental effects of marine renewable energy development around the world, pp. 224, 2016.
[10] P. Mycek, B. Gaurier, G. Germain, G. Pinon, E. Rivoalen, Experimental study of the turbulence intensity effects on marine current turbines behaviour. Part I: one single turbine, Renew. Energy 66 (2014a) 729–746.
[11] P. Mycek, B. Gaurier, G. Germain, G. Pinon, E. Rivoalen, Experimental study of the turbulence intensity effects on marine current turbines behaviour. Part II: two interacting turbines, Renew. Energy 68 (2014b) 876–892.
[12] L. Myers, A. Bahaj, Experimental analysis of the flow field around horizontal axis tidal turbines by use of scale mesh disk rotor simulators, Ocean. Eng. 37 (2–3) (2010) 218–227.
[13] L. Myers, A. Bahaj, An experimental investigation simulating flow effects in first generation marine current energy converter arrays, Renew. Energy 37 (1) (2012) 28–36.
[14] L. Chen, W. Lam, Slipstream between marine current turbine and seabed, Energy 68 (2014) 801–810.
[15] A.J.G. Brown, S.P. Neill, M.J. Lewis, Tidal energy extraction in three-dimensional ocean models, Renew. Energy (2017).
[16] R. O'Hara Murray, A. Gallego, A modelling study of the tidal stream resource of the pentland firth, scotland, Renew. Energy 102 (2017) 326–340.
[17] J. van der Molen, P. Ruardij, N. Greenwood, Potential environmental impact of tidal energy extraction in the Pentland Firth at large spatial scales: results of a biogeochemical model, Biogeosciences 13 (2016) 2593–2609.
[18] I. Fairley, I. Masters, H. Karunarathna, The cumulative impact of tidal stream turbine arrays on sediment transport in the Pentland Firth, Renew. Energy 80 (2015) 755–769.
[19] R. Martin-Short, J. Hill, S. Kramer, A. Avdis, P. Allison, M. Piggott, Tidal resource extraction in the Pentland Firth, UK: potential impacts on flow regime and sediment transport in the Inner Sound of Stroma, Renew. Energy 76 (2015) 596–607.
[20] J. Thiébot, P.B. du Bois, S. Guillou, Numerical modeling of the effect of tidal stream turbines on the hydrodynamics and the sediment transport–Application to the Alderney Race (Raz Blanchard), France, Renew. Energy 75 (2015) 356–365.
[21] Z. Yang, T. Wang, A. Copping, S. Geerlofs, Modeling of in-stream tidal energy development and its potential effects in Tacoma Narrows, Washington, USA. Ocean Coast. Manag. 99 (2014) 52–62.
[22] P. Robins, S. Neill, M. Lewis, Impact of tidal-stream arrays in relation to the natural variability of sedimentary processes, Renew. Energy 72 (2014) 311–321.
[23] V. Ramos, R. Carballo, M. Álvarez, M. Sánchez, G. Iglesias, Assessment of the impacts of tidal stream energy through high-resolution numerical modeling, Energy 61 (2013) 541–554.
[24] D. Plew, C. Stevens, Numerical modelling of the effect of turbines on currents in a tidal channel - Tory Channel, New Zealand, Renew. Energy 57 (2013) 269–282.
[25] R. Ahmadian, R. Falconer, B. Bockelmann-Evans, Far-field modelling of the hydro-environmental impact of tidal stream turbines, Renew. Energy 38 (1) (2012) 107–116.
[26] S.P. Neill, J.R. Jordan, S.J. Couch, Impact of tidal energy converter (TEC) arrays on the dynamics of headland sand banks, Renew. Energy 37 (1) (2012) 387–397.
[27] Z. Defne, K.A. Haas, H.M. Fritz, Numerical modeling of tidal currents and the effects of power extraction on estuarine hydrodynamics along the Georgia coast, USA, Renew. Energy 36 (12) (2011) 3461–3471.
[28] D. Hasegawa, J. Sheng, D.A. Greenberg, K.R. Thompson, Far-field effects of tidal energy extraction in the Minas Passage on tidal circulation in the Bay of Fundy and Gulf of Maine using a nested-grid coastal circulation model, Ocean. Dyn. 61 (11) (2011) 1845–1868.
[29] G. Shapiro, Effect of tidal stream power generation on the region-wide circulation in a shallow sea, Ocean Sci. 7 (1) (2011) 165–174.
[30] R. Karsten, J. McMillan, M. Lickley, R. Haynes, Assessment of tidal current energy in the Minas passage, Bay of Fundy, Proc. Inst. Mech. Eng. Part A J. Power Energy 222 (5) (2008) 493–507.
[31] The Crown Estate, UK wave and tidal key resource areas project–Summary report, 2012.
[32] Black, Veatch, Phase II. UK Tidal Stream energy resource assessment. Carbon Trust Marine Energy Challenge, 2005.
[33] S. Salter, J.M. Taylor, Vertical-axis tidal-current generators and the Pentland Firth, Proc. Inst. Mech. Eng. Part A J. Power Energy 221 (2) (2007) 181–199.
[34] C. Chen, H. Liu, R.C. Beardsley, An unstructured grid, finite-volume, three-dimensional, primitive equations ocean model: application to coastal ocean and estuaries, J. Atmos. Ocean. Technol. 20 (1) (2003) 159–186.
[35] J. Wolf, N. Yates, A. Brereton, H. Buckland, M. De Dominicis, A. Gallego, R. O'Hara Murray, The Scottish Shelf Model. Part 1: shelf-wide domain, Scott. Mar. Freshw. Sci. 7 (3) (2016) 151.
[36] H. Burchard, Applied turbulence modelling in marine waters, vol. 100, Springer Science & Business Media, 2002.
[37] J. Smagorinsky, General circulation experiments with the primitive equations: I. the basic experiment, Mon. Weather Rev. 91 (3) (1963) 99–164.
[38] D.P. Dee, S.M. Uppala, A.J. Simmons, P. Berrisford, P. Poli, S. Kobayashi, U. Andrae, M.A. Balmaseda, G. Balsamo, P. Bauer, P. Bechtold, A.C.M. Beljaars, L. van de Berg, J. Bidlot, N. Bormann, C. Delsol, R. Dragani, M. Fuentes, A.J. Geer, L. Haimberger, S.B. Healy, H. Hersbach, E.V. Hlm, L. Isaksen, P. Kllberg, M. Khler, M. Matricardi, A.P. McNally, B.M. Monge-Sanz, J.-J. Morcrette, B.-K. Park, C. Peubey, P. de Rosnay, C. Tavolato, J.-N. Thpaut, F. Vitart, The ERA-Interim reanalysis: configuration and performance of the data assimilation system, Q. J. R. Meteorol. Soc. 137 (656) (2011) 553–597.
[39] C.W. Fairall, E.F. Bradley, D.P. Rogers, J.B. Edson, G.S. Young, Bulk parameterization of air-sea fluxes for tropical ocean-global atmosphere coupled-ocean atmosphere response experiment, J. Geophys. Res. Oceans 101 (C2) (1996b) 3747–3764.
[40] C. Fairall, E.F. Bradley, J. Godfrey, G. Wick, J.B. Edson, G. Young, Cool-skin and warm-layer effects on sea surface temperature, J. Geophys. Res. 101 (C1) (1996a) 1295–1308.
[41] K. Edwards, R. Barciela, M. Butenschon, Validation of the NEMO-ERSEM operational ecosystem model for the North West European continental shelf, Ocean Sci. 8 (2012) 983–1000.
[42] E. O'Dea, A. Arnold, K. Edwards, R. Furner, P. Hyder, M. Martin, J. Siddorn, D. Storkey, J. While, J. Holt, H. Liu, An operational ocean forecast system incorporating NEMO and SST data assimilation for the tidally driven European North-West shelf, J. Oper. Oceanogr. 5 (1) (2012) 3–17.
[43] G. Madec, the NEMO team, NEMO ocean engine - version 3.6 stable: Note du pole de modélisation No 27, Institut Pierre-Simon Laplace (IPSL), 2016. ISSN No 1288–1619.
[44] G.D. Egbert, S.Y. Erofeeva, Efficient inverse modeling of barotropic ocean tides, J. Atmos. Ocean. Technol. 19 (2) (2002) 183–204.
[45] T. Adcock, A. Borthwick, G. Houlsby, The open boundary problem in tidal basin modelling with energy extraction. in: Proceedings of the 9th European Wave and Tidal Energy Conference, Southampton, UK, 2011.
[46] C. Garrett, D. Greenberg, Predicting changes in tidal regime: the open boundary problem, J. Phys. Oceanogr. 7 (2) (1977) 171–181.
[47] V. Bell, A. Kay, R. Jones, R. Moore, Development of a high resolution grid-based river flow model for use with regional climate model output, Hydrol. Earth Syst. Sci. 11 (1) (2007) 532–549.
[48] V. Bell, A. Kay, R. Jones, R. Moore, N. Reynard, Use of soil data in a grid-based hydrological model to estimate spatial variation in changing flood risk across the UK, J. Hydrol. 377 (3) (2009) 335–350.
[49] S.J. Cole, R.J. Moore, Distributed hydrological modelling using weather radar in gauged and ungauged basins, Adv. Water Resour. 32 (7) (2009) 1107–1120.
[50] Z. Yang, T. Wang, A.E. Copping, Modeling tidal stream energy extraction and its effects on transport processes in a tidal channel and bay system using a three-dimensional coastal ocean model, Renew. Energy 50 (2013) 605–613.
[51] S. Baston, S. Waldman, J. Side, Modelling energy extraction in tidal flows, in: TeraWatt Position Papers. MASTS, Ch. 4, 2015, pp. 75–107.
[52] B. Polagye, J. Thomson, Tidal energy resource characterization: methodology and field study in Admiralty Inlet, Puget Sound, WA (USA), Proc. Inst. Mech. Eng. Part A J. Power Energy 227 (3) (2013) 352–367.
[53] R. Bedard, M. Previsic, B. Polagye, G. Hagerman, A. Casavant, North America tidal in-stream energy conversion technology feasibility study, EPRI Report TP008, 2006.
[54] The Scottish Government, Scotland's national marine plan, 2015. http://www.gov.scot/Publications/2015/03/6517.
[55] The Crown Estate, Pentland Firth and Orkney Waters strategic area review project, 2013.
[56] I. Robinson, The tidal dynamics of the Irish and Celtic Seas, Geophys. J. Int. 56 (1) (1979) 159–197.
[57] D.T. Pugh, Tides, Surges and Mean Sea-level (Reprinted with Corrections), John Wiley & Sons Ltd, 1996.
[58] A. Grinsted, S. Jevrejeva, R.E. Riva, D. Dahl-Jensen, Sea level rise projections for northern Europe under RCP8. 5, Clim. Res. 64 (1) (2015) 2015.
[59] L. Kregting, B. Elsaesser, R. Kennedy, D. Smyth, J. O'Carroll, G. Savidge, Do changes in current flow as a result of arrays of tidal turbines have an effect on benthic communities? PloS one 11 (8) (2016), e0161279.
[60] J. Holt, S. Wakelin, J. Lowe, J. Tinker, The potential impacts of climate change on the hydrography of the northwest European continental shelf, Prog. Oceanogr. 86 (3) (2010) 361–379.
[61] J. Holt, L. Umlauf, Modelling the tidal mixing fronts and seasonal stratification of the Northwest European continental shelf, Cont. Shelf Res. 28 (7) (2008) 887–903.
[62] R. Pingree, D. Griffiths, Tidal fronts on the shelf seas around the British Isles, J. Geophys. Res. Oceans 83 (C9) (1978) 4615–4622.
[63] J. Simpson, D. Bowers, Models of stratification and frontal movement in shelf seas, Deep Sea Res. Part A. Oceanogr. Res. Pap. 28 (7) (1981) 727–738.
[64] J. Simpson, J. Hunter, Fronts in the Irish Sea, Nature 250 (1974) 404–406.
[65] R. Pingree, G. Mardell, P. Holligan, D. Griffiths, J. Smithers, Celtic Sea and Armorican current structure and the vertical distributions of temperature and chlorophyll, Cont. Shelf Res. 1 (1) (1982) 99–116.
[66] K. Richardson, A. Visser, F.B. Pedersen, Subsurface phytoplankton blooms fuel pelagic production in the North Sea, J. Plankton Res. 22 (9) (2000) 1663–1671.
[67] B. Scott, J. Sharples, O.N. Ross, J. Wang, G.J. Pierce, C. Camphuysen, Sub-surface hotspots in shallow seas: fine-scale limited locations of top predator foraging habitat indicated by tidal mixing and sub-surface chlorophyll, Mar. Ecol. Prog. Ser. 408 (2010) 207–226.
[68] P.I. Miller, S. Christodoulou, Frequent locations of oceanic fronts as an indicator of pelagic diversity: application to marine protected areas and renewables, Mar. Policy 45 (2014) 318–329.

[69] M. Stramska, T.D. Dickey, Phytoplankton bloom and the vertical thermal structure of the upper ocean, J. Mar. Res. 51 (4) (1993) 819–842.
[70] J. Holt, R. Proctor, The seasonal circulation and volume transport on the Northwest European continental shelf: a fine-resolution model study, J. Geophys. Res. Oceans 113 (C6) (2008).
[71] OSPAR Commission, Quality Status Report 2000, Region II: Greater North Sea, OSPAR Commission, London, 2000, 136 + xiii pp.
[72] W. Turrell, G. Slesser, R. Payne, R. Adams, P. Gillibrand, Hydrography of the east Shetland basin in relation to decadal North Sea variability, ICES J. Mar. Sci. 53 (6) (1996) 899–916.
[73] E. Svendsen, R. Sætre, M. Mork, Features of the northern North Sea circulation, Cont. Shelf Res. 11 (5) (1991) 493–508.
[74] H. Neumann, I. de Boois, I. Kröncke, H. Reiss, Climate change facilitated range expansion of the non-native Angular crab Goneplax rhomboides into the North Sea, Mar. Ecol. Prog. Ser. 484 (2013) 143–153.
[75] H. Neumann, S. Ehrich, I. Kröncke, Variability of epifauna and temperature in the northern North Sea, Mar. Biol. 156 (9) (2009) 1817–1826.
[76] A. Shields, Application of Similarity Principles and Turbulence Research to Bed-load Movement, Soil Conservation Service, 1936.
[77] R. Soulsby, Dynamics of marine sands: A manual for practical applications, Thomas Telford, 1997.
[78] J. Aldridge, E. Parker, L. Bricheno, S. Green, J. van der Molen, Assessment of the physical disturbance of the northern European continental shelf seabed by waves and currents, Cont. Shelf Res. 108 (2015) 121–140.
[79] M. Heath, A. Sabatino, N. Serpetti, C. McCaig, R. O'Hara Murray, Modelling the sensitivity of suspended sediment profiles to tidal current and wave conditions, Ocean Coast. Manag. (2016).
[80] A. Chatzirodou, H. Karunarathna, D.E. Reeve, Investigation of deep sea shelf sandbank dynamics driven by highly energetic tidal flows, Mar. Geol. 380 (2016) 245–263.
[81] Department for Business, Energy & Industrial Strategy, Electricity: Chapter 5, Digest of United Kingdom Energy Statistics (DUKES), 2016. https://www.gov.uk/government/statistics/electricity-chapter-5-digest-of-united-kingdom-energy-statistics-dukes.
[82] S.W. Funke, P.E. Farrell, M. Piggott, Tidal turbine array optimisation using the adjoint approach, Renew. Energy 63 (2014) 658–673.
[83] S. Cox, M. Witt, C. Embling, B. Godley, P. Hosegood, P. Miller, S. Votier, S. Ingram, Temporal patterns in habitat use by small cetaceans at an oceanographically dynamic marine renewable energy test site in the Celtic Sea, Deep Sea Res. Part II Top. Stud. Oceanogr. 141 (2017) 178–190.
[84] D. Sadykova, B. Scott, M. De Dominicis, S. Wakelin, A. Sadykov, J. Wolf, Bayesian joint models with INLA exploring marine mobile predator-prey and competitor species habitat overlap, Ecol. Evol. (2017).